ARTICLE

Sympatric and allopatric evolutionary contexts shape differential immune response in *Biomphalaria / Schistosoma* interaction.

Anaïs PORTET[1], Silvain PINAUD[1], Cristian CHAPARRO[1], Richard GALINIER[1], Guillaume M. CHARRIERE[2], Jean-François ALLIENNE[1], David DUVAL[1], Benjamin GOURBAL[1§]

[1] Univ. Perpignan Via Domitia, Interactions Hôtes Pathogènes Environnements UMR 5244, CNRS, IFREMER, Univ. Montpellier, F-66860 Perpignan, France

[2] Interactions Hôtes-Pathogènes-Environnements (IHPE), UMR 5244, CNRS, Ifremer, Université de Perpignan Via Domitia, Université de Montpellier, Montpellier, 34095, France.

[§] corresponding author:

Benjamin Gourbal

UMR5244 IHPE, Université de Perpignan

58 avenue Paul Alduy, 66860 Perpignan

benjamin.gourbal@univ-perp.fr

Abstract

Background:

Selective pressures between hosts and their parasites can results in reciprocal evolution or adaptation of specific life history traits. Local adaptation of resident hosts and parasites should lead to host-parasite systems performing better in sympatry when compared to allopatry. Between-population variations in parasite infectivity/virulence and host defense/resistance, referring as compatibility phenotype, were often the proxy used to analyse sympatric or allopatric adaptation. Nevertheless, some reported cases exist where allopatric host-parasite systems demonstrate compatibility phenotypes similar or greater than the one observed in sympatry. In these cases, the role of local adaptation is questioning. Here, we study the interaction between *Schistosoma* and its vector snail *Biomphalaria* in which such discrepancy in local versus foreign compatibility phenotype has been observed. Herein, we developed an integrative approach to investigate sympatric and allopatric interaction processes and link the underlying molecular mechanisms to the resulting phenotypes. Using comparative "omics" approaches joined to analysis of life history traits (immune cellular response, mortality, prevalence and compatibility) we try to bridge the gap of knowledge that exists for connecting local adaptation observations to molecular phenotypes in *Schistosoma/Biomphalaria* interactions.

Results:

We found that despite displaying similar prevalence phenotypes, parasite infection triggered an immune suppression in snails living in sympatry, while it activated an immune response for those living in allopatry. Dual-comparative molecular analyses revealed that parasite infection causes immune suppression in sympatry. miRNAs were used to hijack host's immune response, allowing sympatric parasites to initiate its developmental program earlier and more efficiently.

Conclusions:

We show that despite having similar prevalence phenotypes, sympatric and allopatric snail-*Schistosoma* interactions displayed a strongly different immunobiological molecular dialogue. The ability for allopatric pathogens to adapt rapidly and efficiently to new hosts could have critical consequences on disease emergence and risk of Schistosomiasis outbreaks. These observations would have important consequences in term of Schistosomiasis disease control.

Keywords: sympatry, allopatry, host-parasite compatibility, RNA-seq, immunity

Introduction

Schistosomiasis is the second most widespread human parasitic disease after malaria and affects over 200 million people worldwide (WHO, 2010). *Schistosoma mansoni* (Platyhelminthes, Lophotrochozoa) causes intestinal schistosomiasis. *Schistosoma* needs a mollusc (belonging to *Biomphalaria, Bulinus,* or *Planorbarius* genus) to act as its first intermediate host, where it undergoes part of its life cycle before infecting humans. Patently infected snails support the continuous production of thousands of cercariae, the free-living human-infective stage of the parasite, until dying. Vector snails appeared thus as a central actor of the parasite transmission and thus have deserved greater attention as potential target for Schistosomiasis control. To deserve this objective it is necessary to understand snail-parasite immunobiological interactions and to characterize the molecular mechanisms by which snails and *Schistosoma* interact.

Biomphalaria / Schistosoma compatibility is based on a complex phenotype-to-phenotype or matching-phenotype model (Basch, 1976; Galinier *et al.*, 2017; Mitta *et al.*, 2012; Mitta *et al.*, 2017; Theron *et al.*, 1997; Theron *et al.*, 2014). The success or failure of the infection of *B. glabrata* by *S. mansoni* reflects a complex interplay between the host's defense mechanisms and the parasite's infective strategies. In the past 15 years, the molecular basis of this compatibility polymorphism has been investigated at the genomic (Bonner *et al.*, 2012; Goodall *et al.*, 2006; Tennessen *et al.*, 2015), transcriptomic (Galinier *et al.*, 2017; Ittiprasert *et al.*, 2010; Lockyer *et al.*, 2012; Lockyer *et al.*, 2004; Lockyer *et al.*, 2007; Roger *et al.*, 2008a), proteomic (Bender *et al.*, 2007; Galinier *et al.*, 2013; Hahn *et al.*, 2001; Larson *et al.*, 2014; Mone *et al.*, 2010; Myers *et al.*, 2008; Pila *et al.*, 2016; Roger *et al.*, 2008b) and epigenomic levels (Bridger *et al.*, 2014; Ittiprasert, Knight, 2012; Ittiprasert *et al.*, 2009; Knight *et al.*, 2015; Nelson *et al.*, 2016; Perrin *et al.*, 2012). These studies have revealed that various molecules and pathways involved in immune recognition (snail immune receptors versus parasite antigens), immune effector/anti-effector systems, and immune regulation/activation participate in a complex interplay that governs the match or mismatch of host and parasite phenotypes (Portet *et al.*, 2017). This complex phenotype-by-phenotype interaction (compatibility polymorphism) varies between populations and individuals resulting in a "multi-parasite susceptibility" or "multi-host

infectivity" phenotypes (Theron *et al.*, 2014) that reflect between-population variations in parasite infectivity/virulence and host defense/resistance (Osnas *et al.*, 2015; Tack *et al.*, 2012).

In *B. glabrata/Schistosoma sp.* models, numerous sympatric and allopatric combinations have been tested; (i) different *B. glabrata* laboratory strains (or isolates) show various degrees of susceptibility to *S. mansoni* infection and (ii) different strains of *S. mansoni* display different levels of infectivity towards a particular strain of snail host (Basch, 1976; Prugnolle *et al.*, 2006; Richards, 1975; Theron *et al.*, 1997; Theron *et al.*, 2014). In most cases, interaction in *B.glabrata/Schistosoma* models has been investigated by comparing, (i) sympatric/compatible and (ii) allopatric/incompatible host-parasite associations. Indeed, the general assumption is that the parasites, which have a shorter generation time, larger population sizes and higher reproductive outputs, are ahead in the co-evolutionary conflict against their host and are therefore more likely to locally adapt to them (Frank, 1996; Kawecki, Ebert, 2004). This is exactly what is stated by the “host-parasite local adaptation hypothesis”, in which the sympatric parasite is supposed to perform better than the allopatric one (Ebert, 1994; Kalbe *et al.*, 2016; Kawecki, Ebert, 2004; Lively, 1989). However, it has been observed that compatibility phenotypes between *Biomphalaria* and *Schistosoma* were the same comparing sympatric and allopatric combinations or even greater for allopatric parasites, and thus did not fulfil the "local versus foreign" criterion of the “host-parasite local adaptation hypothesis” (Morand *et al.*, 1996; Osnas, Lively, 2004; Prugnolle *et al.*, 2006). Such compatibility phenotypes have been mostly investigated in terms of parasite infectivity or pathogenicity toward snail hosts, but to our knowledge very few studies have investigated the molecular basis of allopatric compatible interactions from the perspective of both side of the interaction, the host and parasite (Mone *et al.*, 2011; Penczykowski *et al.*, 2015).

Hence, in order to bridge this gap, we herein study sympatric/allopatric interactions displaying similar compatibilities using an integrative approach that links the underlying molecular mechanisms to the resulting phenotypes, based on comparative molecular approaches on both host snails and *Schistosoma* parasites. We set out to analyze the compatibility between South American snail strains (from Recife Brazil and Guacara Venezuela) in combination with three different parasite isolates that displayed nearly the same compatibility phenotype: (i) *S. mansoni* Recife Brazil, (ii) *S. mansoni* Guacara Venezuela (both sympatric and allopatric, narrow geographic scale), and (iii) *S. rodhaini* from Burundi

Africa (allopatric, large geographic and phylogenetic scales). Thus even if compatibility phenotypes (prevalence/intensity) are similar, the characterization of the underlying molecular mechanisms demonstrates a very different immunobiological dialogue between *B. glabrata* vector snails and their sympatric or allopatric *Schistosoma* parasites at the cellular and molecular scales.

To the best of our knowledge very few studies have investigated the molecular basis of local adaptation in host/parasite interactions (Bankers *et al.*, 2018; Robertson *et al.*, 2017). Here we used a powerful global approach to identify the differentially regulated transcripts in snails of a single *B. glabrata* strain under infection by three sympatric or allopatric compatible strains or species of the parasite, *Schistosoma sp.*

Moreover, our results may be of critical importance in terms of Schistosomiasis control. Understanding the mechanisms whereby allopatric parasites efficiently infect host snails, would be mandatory to develop new tools to predict or quantify risks of Schistosomiasis disease outbreaks (Kincaid-Smith *et al.*, 2017).

Materials and Methods

Ethical statements

Our laboratory holds permit # A66040 for experiments on animals, which was obtained from the French Ministry of Agriculture and Fisheries and the French Ministry of National Education, Research, and Technology. The housing, breeding, and care of the utilized animals followed the ethical requirements of our country. The experimenter possesses an official certificate for animal experimentation from both of the above-listed French ministries (Decree # 87–848, October 19, 1987). The various protocols used in this study have been approved by the French veterinary agency of the DRAAF Languedoc-Roussillon (Direction Régionale de l'Alimentation, de l'Agriculture et de la Forêt), Montpellier, France (authorization # 007083).

Biological materials

Two snail strains of *Biomphalaria glabrata* were used in this study: the albino Brazilian strain, (BgBRE) and the Venezuelan strain, (BgVEN). They were exposed to infection by a Brazilian

140 (SmBRE) or Venezuelan (SmVEN) strains of *Schistosoma mansoni*, or by another *Schistosoma*
141 species, *S. rodhaini* (Srod). All host and parasite strains of each different geographical origin were
142 recovered in their native locality and maintain in the laboratory always on their sympatric snail hosts
143 to maintain reciprocal selective pressures and reciprocal sympatric strain adaptation. We housed snails
144 in tanks filled with pond water at 25°C with a 12:12 hour light:dark cycle and supplied ad libitum with
145 fresh lettuce. The Brazilian strain originates from the locality of Recife (east Brazil), the Venezuelan
146 strains of snail and parasite were recovered from the locality of Guacara (north Venezuela) and the
147 African species *Schistosoma rodhaini* originates from Burundi and was obtained from the London
148 British Museum. These *Schistosoma* isolates/species have been selected because they exhibited similar
149 infectivity toward BgBRE or BgVEN strains (see prevalence and intensity in supplementary table S1).
150 Prevalence of SmBRE and SmVEN for the African vector snail *Biomphalaria pfeifferi* from Senegal
151 (BpSEN), and prevalence of the corresponding parasite SmSEN on South American snails were also
152 tested (supplementary table S1).
153
154 ***RNAseq experimental protocol***
155 In order to investigate the molecular response of snails against sympatric and allopatric parasites, a
156 global comparative transcriptomic approach was conducted. One hundred and twenty BgBRE snails
157 were infected with SmBRE, SmVEN or Srod. Each snail was individually exposed for 12 h to 10
158 miracidia in 5mL of pond water. For each experimental infection, 20 snails were recovered at 24 and
159 96 h after infection. The samples were named as follows: BB24, BB96 for BgBRE infected with
160 SmBRE; BV24, BV96 for BgBRE infected with SmVEN; and BR24, BR96 for BgBRE infected with
161 Srod. Two pools of 30 uninfected BgBRE snails (Bre1 and Bre2) were used as controls.
162 - *Whole-snail RNA extraction and sequencing*
163 Total RNA was extracted using TRIZOL® (Sigma Life Science, USA) according to the
164 manufacturer's instructions. Sequencing was performed using in paired-end 72-bp read lengths on
165 Illumina Genome Analyzer II (MGX-Montpellier GenomiX, Montpellier, France).
166 - *De novo transcriptome assembly*
167 *De novo* transcriptome assembly, using all time points, was performed using an in-house pipeline

168 created with the Velvet (1.2.02), Oases (v0.2.04), and CD-HIT-EST (v4.5.4) programs. The assembly
169 of the consensus reference transcriptome was optimized using various parameters, including k-mer
170 length, insert length and expected coverage, as previously described (Dheilly *et al.*, 2015; Pinaud *et*
171 *al.*, 2016). A *de novo* transcriptome was created and contained 159,711 transcripts.

172 - *Differential expression analysis*

173 High-quality reads (Phred score >29) were aligned to the *de novo* transcriptome using Bowtie2
174 (v2.0.2), which was run locally on a Galaxy server. To compare the host responses during the
175 sympatric or allopatric interactions, we used the DESeq2 (v2.12) software to analyse the differential
176 transcript representation between *BgBRE* control strains (uninfected *Bg*BRE1 and *Bg*BRE2) to the
177 sympatric and allopatric conditions (p-value < 0.1) (Pinaud *et al.*, 2016). A Venn diagram was
178 generated using the Venny 2.1 software to highlight which differentially expressed transcripts were
179 specific or common to the different interactions. A heatmap was then created to analyze transcript
180 expression patterns, using log2 Fold Change with Hierarchical Ascending Clustering (HAC) and
181 Pearson correlation (uncentered) as applied by the Cluster (v3.0) and Java TreeView (v1.1.6r4)
182 softwares packages. The differentially represented transcripts were functionally classified using a
183 BlastX analysis with the cut-off set to e-value < $1e^{-3}$ (NCBI dataset; thanks to the Roscoff Data center
184 Cluster, UPMC) and gene ontology was assigned using an automatic annotation, Blast2GO (v3.0.8)
185 (supplementary table S2). Based on automatic annotation and functional domains and according to the
186 literature we identified the potential immune transcripts involved in snail immunity.

187

188 ***Schistosoma intra-molluscal stage transcriptome analysis: Dual RNA-seq***

189 Host response against pathogens constitutes solely one side of the molecular dialogue occurring in
190 host/parasite interactions. To analyse all the complexity of such dialogue, the parasite response into
191 host tissue needs also to be investigated. Herein a dual RNA-seq approach was thus conducted to gain
192 in a broader understanding of sympatric and allopatric host/parasite interactions.

193 - <u>*Schistosome read selection*</u>

194 The *Biomphalaria* (v1) and *Schistosoma* (v5.2) genomes have been concatenated
195 (https://www.vectorbase.org/organisms/biomphalaria-glabrata;

196 http://www.sanger.ac.uk/resources/downloads/helminths/schistosoma-mansoni.html). High quality
197 reads (Phred score >29) were mapped against these concatenated genomes using Bowtie2 (v2.0.2),
198 which was run locally on the Galaxy project server. The reads that mapped only once and exclusively
199 to the *Schistosoma* genome were collected as corresponding to *Schistosoma* reads; reads that mapped
200 to the *Biomphalaria* genome or more than once to either genomes were removed from the analysis.

201 - <u>*Gene analysis*</u>

202 The above-selected *Schistosoma* reads were mapped against the concatenate genome to identify intra-
203 molluscal stage-specific *Schistosoma* genes. In order to select the relevant genes, the reads mapped in
204 all experimental conditions were summed. Solely genes with a minimal sum of 10 reads were kept for
205 the analysis. A heatmap was generated to analyse *Schistosoma* gene expression patterns using
206 Hierarchical Ascending Clustering (HAC) with Pearson correlation (uncentered) as applied by the
207 Cluster (v3.0) and Java TreeView (v1.1.6r4) software packages. Functional annotation of the genes
208 was assigned using BlastX with the cut-off set to e-value < $1e^{-3}$ (NCBI dataset, local cluster) and gene
209 ontology was performed using Blast2GO (v4.0.7) (supplementary table S3).

210

211 ***Innate immune cellular response analysis: microscopy and flow cytometry***

212 Hemocytes appeared as the main cells supporting *Biomphalaria* snail immune response. Thus, to go
213 further in the description of snail response against parasites, quantitative and qualitative changes in
214 hemocyte populations were investigated. For this purpose, BgBRE and BgVEN snails were used.
215 Snails were infected as described above, using either SmBRE or SmVEN parasites. For each
216 experimental infection, snails were recovered at 24 and 96 h after infection, and designated as follows:
217 BB24 and BB96 for BgBRE infected with SmBRE; BV24 and BV96 for BgBRE infected with
218 SmVEN; VV24 and VV96 for BgVEN infected with SmVEN; and VB24 and VB96 for BgVEN
219 infected with SmBRE. Snails of each strain, BgBRE and BgVEN, were recovered and used as
220 controls.

221 - <u>Hemocyte proliferation analysis: microscopy</u>

222 Microscopic inspection of hemocyte proliferation was conducted using 12 infected BgBRE (6
223 BgBRExSmBRE and 6 BgBRExSmVEN) and 3 uninfected BgBRE snails. The hemocytes of 3 snails

224 (biological replicates) were counted for each condition at 24h and 96h after infection. The
225 proliferation of circulating hemocytes was studied by using a Click-iT EdU Alexa Fluor 488 Flow
226 Imaging Kit (Molecular Probes). At each time point, circulating hemocytes were recovered by direct
227 puncture after foot retraction and 1mM of EdU solution was added to the hemolymph. Three hours
228 later, the amount of EdU incorporated by the circulating hemocytes was visualized *in-vitro* after
229 fixation of the cells and performing a covalent coupling of Alexa Fluor 488 to the EdU residues trough
230 a click chemistry reaction flowing manufacturer indications, then nuclei of hemocytes were
231 counterstained with DAPI (Biotum) staining, and the sample was analysed on a confocal microscope
232 using a Zeiss LSM 700, with 4 lasers (405, 488, 555 and 633 nm). Positive cells were counted and
233 between-sample differences in the percentage of proliferation were tested using a Fisher exact test,
234 with significance accepted at p-value<0.05.

235 - Hemocyte proliferation and population profiles analysis: flow cytometry

236 Qualitative changes in hemocyte populations following infection by sympatric or allopatric parasites
237 were studied using a flow cytometry approach. For this 72 infected BgBRE or BgVEN (36 infected by
238 SmBRE and 36 infected by SmVEN) and 18 uninfected BgBRE or BgVEN snails were used. Six
239 biological replicates (pools of 3 snails per replicate) were performed for each condition. Flow
240 cytometry was used to profile and assess the proliferation of circulating hemocytes using Click-
241 iTEdUAlexa Fluor 647 labelling (Molecular Probes). At each time point, 1mM of EdU solution was
242 injected into pericardial cavity of each snail. Three hours later six replicates of 3 snails were collected,
243 and the hemolymph was extracted from the head-foot according to standard procedures (Sminia,
244 Barendsen, 1980). The hemolymph was pooled from the three snails, and 100 µl were subjected to
245 analysis with the above-listed kit, according to the manufacturer's instructions. The percentage of
246 proliferative cells was calculated by flow cytometry.

247 The hemocytes were profiled along the course of infection using Side Scatter Chanel (SSC) to
248 estimate cell granularity and Forward Scatter Chanel (FSC) to estimate cell size. The cell repartition
249 along these two parameters enables to identify cell sub-populations. The flow cytometry was
250 performed using a FACS Canto from BD Biosciences (RIO Imaging Platform, Montpellier, France).
251 For each sample, 10,000 events were counted. The results were analyzed with the FlowJo V 10.0.8

252 software. Between-group differences in the percent of proliferation were tested using the Mann-
253 Whitney U-test, with significance accepted at p-value<0.05.
254
255 ***Histological procedures***
256 A histological approach was conducted in order to investigate differences in miracidia to sporocyst
257 development, while comparing sympatric and allopatric parasite growth, development and maturation
258 into snail tissues. BgBRE snails (n=8 per group) were infected as described above with either SmBRE
259 (sympatric) or SmVEN (allopatric) parasites. At 24 and 96 h after infection, two snails were fixed in
260 Halmi's fixative (4.5% mercuric chloride, 0.5% sodium chloride, 2% trichloroacetic acid, 20% formol,
261 4% acetic acid and 10% picric acid-saturated aqueous solution). Embedding in paraffin and transverse
262 histological sections (3-μm) were performed using the RHEM platform (Montpellier, France)
263 facilities. The slides were stained using Heidenhain's azan trichromatic staining solution as follows:
264 (i) serial re-hydration was performed in toluene followed by 95%, 70%, and 30% ethanol and then
265 distilled water; (ii) coloration was performed using azocarmine G (70% ethanol, 1% aniline, 1% acetic
266 alcohol, distilled water, 5% phosphotungstic acid, distilled water, Heidenhain's azan) and (iii) serial
267 dehydration was performed using 95% ethanol, absolute ethanol, and toluene. The preparations were
268 then mounted with Entellan (Sigma Life Science, St. Louis Missouri, USA) and subjected to
269 microscopic examination. The parasite sizes were measured with the ImageJ software (v2.0.0), and
270 between-group size differences were tested using the Mann-Whitney U-test with statistical
271 significance accepted at a p-value<0.05 based on the mean of the three largest serial cuts of each
272 sporocyst in sympatric or allopatric conditions.
273
274 **In-silico *characterization of* Schistosoma *miRNAs***
275 Parasites may communicate or interfere with their host using different strategies based mainly on
276 excreted/secreted products released into hemolymph. In this context, miRNAs appeared as the most
277 relevant mean of communication that can be used by parasites. To test for such hypothesis *S. mansoni*
278 miRNAs were analyzed *in-silico* by comparing the relevant miRNA database (miRBase) to our
279 RNAseq libraries generated at the 24h following sympatric or allopatric infections. S. *mansoni*

280 precursor sequences were downloaded from miRBase (http://www.mirbase.org, 03/09/2017), and
281 high-quality reads from naive (BgBRE) and 24 h post-infection samples (BB24, BV24, BR24) were
282 aligned against a *S. mansoni* sub-database of miRBase, as previously described (Zhao *et al.*, 2016).
283 The identified precursors were confirmed by alignment of high-scoring reads onto precursor and
284 mature miRNAs from miRBase. Solely reads with 100% identity were retained for analysis. The
285 localization of each read against miRNA sequence allowed us to identify either the precursor or just
286 the mature miRNA. Precursors found under both naive and infected conditions were excluded to retain
287 exclusively the miRNAs present in samples from infected snails and avoid cross-species
288 contamination because of the potential conserved features of miRNAs from *B. glabrata* and *S.*
289 *mansoni*.
290 Putative miRNA targets were predicted from among the differentially represented immune-related
291 transcripts (figure 1) using Miranda tools (using parameters: Miranda input_miRinput_Transcriptome
292 -out results.txt -quiet -sc 140 -en -15) (Enright *et al.*, 2003). Because mature miRNAs may exist in two
293 forms depending on which strand (5'-3') of the precursor stem-loop is maturated the predicted
294 interactions could involve the 5' and/or 3' forms, as noted. The results were extracted using the awk
295 tool, listed in supplementary files (supplementary table S4), and used to generate a Venn diagram. To
296 confirm the ability of a selected pre-miRNA to produce the stem-loop necessary to produce the mature
297 form, the secondary structures of precursor were predicted using RNA structure Web tool
298 (http://rna.urmc.rochester.edu/RNAstructureWeb, 03/09/2017) using default parameters.
299
300 ***Snail survival analysis***
301 Allopatric or sympatric parasites could have different levels of virulence or impacts on their host that
302 could impair snail survival. To test for such discrepancy we investigated the mortality rates of infected
303 snails over the course of sympatric or allopatric infections. One hundred and sixty BgBRE snails were
304 infected as described above with SmBRE or SmVEN strains (n=50), and 60 non-infected BgBRE
305 snails were retained as controls. The numbers of dead snails were compiled weekly for 14 weeks. A
306 Kaplan-Meier estimator was used to estimate the survival function from lifetime data. Survival curves
307 were generated using the xlstats Mac software and the log-rank test was applied with significance

308 accepted at $p<0.05$.

309

310 **Results**

311 ***A whole-snail transcriptomic approach for investigating the molecular basis of the innate immune***
312 ***response in the sympatric and allopatric contexts***

313 The global transcript representation was analyzed using the previously described RNAseq pipeline
314 developed in our laboratory (Dheilly *et al.*, 2015; Galinier *et al.*, 2017; Pinaud *et al.*, 2016). The
315 *Bg*BRE snail host had the same prevalence and intensity phenotypes when exposed to *Sm*BRE,
316 *Sm*VEN or *S*rod parasites (see Table S1). Of the 159,711 transcripts of the *Bg*BRE transcriptome,
317 3,865 (2.4%) were differentially represented in all sympatric and allopatric conditions compared to
318 naive snails (table 1, supplementary fig. S1). We performed automatic Blast2GO annotation, discarded
319 the non-annotated transcripts, and retained 1,017 annotated transcripts (26.3% of the differentially
320 represented transcripts). Finally, as we were interested in the innate immune response of the snail to
321 the sympatric and allopatric parasites, we focused on transcripts known to have immune-related
322 functions. Of the annotated differentially expressed transcripts, 336 were identified as being immune-
323 related; this subset corresponded to 8.7% of all differentially represented transcripts. The heatmap
324 generated for all differentially represented transcripts is presented in supplementary fig. S1.

325

326 Venn diagrams were used to highlight the relationships of the transcripts that were differentially
327 represented in the *B. glabrata* and *Schistosoma sp.* interactions. Overall, 189, 180, and 164 transcripts
328 were differentially represented in the BB (BgBRE/SmBRE, sympatric), BV (BgBRE/SmVEN,
329 allopatric), and BR (BgBRE/Srod, allopatric) interactions, respectively (fig. 1A). Of the selected
330 transcripts, 40 were shared by the BB, BV and BR interactions (fig. 1A), and displayed globally the
331 same differentially expressed pattern of expression (fig. 1B, cluster 1). These transcripts may
332 correspond to the snail's basal immune response against *Schistosoma* parasites.

333 Of the 140 transcripts exclusive to the sympatric (BB) interaction, which represented 74.1% of the
334 immune transcripts found to be differentially represented in this interaction (fig. 1A), 100% were

335 under-represented at 24 h post-infection, and 74.6% of these transcripts were observed exclusively at
336 this time point (fig. 1B, cluster 5).
337 Very similar transcript expression patterns were observed for the two allopatric interactions (BV and
338 BR). Clusters 6 and 7, comprising only 28 and 11 transcripts, were exclusive to BV and BR,
339 respectively. In BV interaction (fig. 1B, cluster 6), at 96 h after infection 96.5% of the transcripts were
340 expressed: 22% over-represented. In BR interaction (fig. 1B, cluster 7), 100% of the transcripts were
341 expressed at 96 h after infection: 82% over-represented. Of the 108 transcripts shared by BV and BR
342 (cluster 3, representing 60% and 65.9 % of the transcripts, respectively) (fig. 1A; fig. 1B, cluster 3),
343 98.1% were expressed at 96 h post-infection: 28.2% over-represented (fig. 1B, cluster 3).
344 Altogether, these results show that the host immune-related transcriptomic response differed widely
345 between the sympatric and allopatric interactions. All of the differentially represented transcripts were
346 under-expressed at 24 h after infection in sympatry, while the differentially represented transcripts in
347 alloparty were mostly over-expressed at 96 h after infection. Moreover, the sympatric interaction was
348 associated with a strong immunosuppression (fig. 1B, cluster 5), whereas allopatry yielded an
349 activation of the immune response (fig. 1B, cluster 3).
350 We decided to explore the function of differentially regulated transcripts between the sympatric and
351 allopatric interactions in order to investigate if these differentially regulated transcripts belong to
352 different functional categories. For that, we performedan automatic annotation with Blast2GO
353 (supplementary table S2). Based on automatic annotation and according to the literature we distributed
354 the relevant differentially expressed immune transcripts into three groups: (i) immune recognition
355 molecules, (ii) immune effectors, and (iii) immune signalling molecules (fig. 1C). Then these three
356 groups were subdivided into functional categories (fig. 2). In the BB sympatric interaction, immune
357 recognition molecules, immune effectors and immune signalling pathways correspond to 13.1%,
358 18.3% and 4.2%, respectively (sums of all relevant transcripts at all infection time points). Among the
359 transcripts distributed into these groups, 89.0% were under-represented. In the BV allopatric
360 interaction, the three groups corresponded respectively to 10.8%, 12.9% and 8.6% and among them
361 65.9% were under-represented. Finally, in the BR allopatric interaction, they correspond to 12%,
362 12.5% and 7.8% and 62.5% of them were under-represented. When we compared the percentage of

363 each immunological group in the sympatric and allopatric interactions, no specific functional subset
364 was particularly repressed in the BB sympatric interaction (fig. 1C; fig. 2). In fact, most of the time the
365 same immune functions were affected in sympatric and allopatric infections but different immune
366 transcripts (grey and black diamond in fig. 2) showed differential regulation following infections (fig.
367 2).
368 The differentially regulated transcripts belonging to the three immunological groups (fig. 2) were
369 largely involved in immune cellular responses, cell adhesion, extra cellular matrix component, cell
370 migration, cell differentiation and cell proliferation. All of these functions were under-represented in
371 sympatric interaction (76%), whereas many were over-represented in allopatric ones (39%) at 24h
372 after infections (fig. 2).
373
374 ***Immune cellular responses in the sympatric and allopatric contexts***
375 As the transcriptomic approach indicated that multiple immunobiological functions seem to be altered
376 in the host response during the interaction with the parasites, we next investigated whether differences
377 in immune responses in sympatric versus allopatric infections could be seen at the cellular level.
378 Hemocytes, the snail immune cells, participate directly in the immune response against the parasites,
379 and immune cell activation under an immunological challenge can translate into cell proliferation
380 and/or cell morphology modifications.
381 Thus to investigate such immune cell activation, cell proliferation was quantified using EdU nuclear
382 labelling (fig. 3). EdU is a nucleoside analogue of thymine incorporated into DNA during DNA
383 synthesis. This incorporation reflects the mitotic activity of hemocytes. As the two tested allopatric
384 interactions appeared extremely similar at the transcriptomic level, we compared only the BV
385 (allopatric) interaction and BB (sympatric) interaction for further analyses. Circulating hemocytes
386 recovered in snail hemolymph were EdU-labelled *in-vitro* to identify mitotic circulating hemocytes
387 (fig. 3A). Edu-positive hemocytes were quantified using confoncal microscopy and showed that
388 hemocyte proliferation was induced by 3 fold following *Schistosoma* infection in BV compared to BB
389 (fig. 3B). Twenty-four hours after infection, proliferative circulating cells increase significantly in BV,
390 with 5.2% of proliferative cells compared to BB with 2.6% (Fisher exact test two-tailed $p = 7.6\ e10^{-6}$)

391 (fig. 3B). Moreover, this result demonstrates for the first time that "circulating" hemocytes are able to
392 proliferate following *Schistosoma* infections.
393
394 Hemocyte proliferation was assessed using flow cytometry after *in-vivo* EdU-labelling (fig. 4A). At
395 24h after infection, the rate of proliferating cells was increased significantly (Mann Whitney U test:
396 U=36; z = -2.8; p = 0.0022) by more than two fold between the allopatric and sympatric interactions,
397 4.2% compared to 1.8% respectively. At 96 h after infection, there were fewer proliferating cells: the
398 percentage of proliferating hemocytes was similar in sympatric BB interaction compared to the control
399 (1%, Mann Whitney U test: U=17; z=-0.27; p = 0.3936), while remaining somewhat higher in
400 allopatric BV interaction (2.3%, Mann Whitney U test: U=0; z=2.65; p = 0.009).
401 To confirm that our observations were related to the type of interaction rather than to a strain effect,
402 we performed the same experiments using another *Biomphalaria glabrata* strain, BgVEN as the host
403 and SmVEN and SmBRE as the sympatric and the allopatric parasite, respectively (fig. 4B). The rate
404 of proliferating hemocytes increased significantly (Mann Whitney U test: U=36; z=-2.8; p = 0.0022)
405 by more than 3 fold between the allopatric (VB: BgVEN/SmBRE) and the sympatric (VV:
406 BgVEN/SmVEN) interactions at 24 h after infection (6.8% compared to 2.0% respectively). At 96 h
407 after infection, both rates were decreased, albeit more for VV (0.1%, Mann Whitney U test: U=2;
408 z=2.48; p = 0.013) than for VB (2.7%, Mann Whitney U test: U=36; z=2.8; p = 0.0022). These results
409 similar to the one observed for BgBRE interactions confirmed that the effects observed at the cellular
410 level were related to the type of interactions (sympatric versus allopatric) rather than to the host or
411 parasite strains used.
412
413 In addition to the mitotic activity, hemocyte morphology was estimated using flow cytometry by
414 measuring their size and granularity. We analyzed the circulating hemocyte populations in non-
415 infected versus infected snails in two *B. glabrata* snail strains (BgBRE and BgVEN) in sympatric and
416 allopatric interactions with parasites (fig. 4C and 4D). Morphology and heterogeneity of circulating
417 hemocytes varied in a similar manner between BgBRE and BgVEN snails subjected to infection (fig.
418 4C and 4D) and we observed infection-related differences in cell morphology. In non-infected snails,

419 the content of circulating hemocytes was very heterogeneous, but appeared to represent a single
420 population that exhibited a continuous gradient of size and granularity (fig. 4C and 4D), which is
421 typical of *B. glabrata* hemocytes (Baeza Garcia *et al.*, 2010). However, hemocyte population
422 heterogeneity changed quickly after infection. In allopatric interactions, 24 h after infection (fig. 4C,
423 BV24, and 4D, VB24) two populations could be distinguished: a population P1 (corresponding to that
424 seen in non-infected snails) and a population P2 (a new population). P2 cells exhibited increased
425 granularity, retained a high degree of size variability, and showed a mitotic activity, as indicated by
426 EdU labeling (fig. 4C and 4D, red dots). This profile was transitory, with the P2 population
427 disappearing by 96 h after infection (fig. 4C, BV96, and 4D, VB96). Altogether, these results show
428 that, upon infection, the snail circulating immune cells exhibit a particular population dynamics with
429 transient increase of the mitotic activity associated with morphology modifications that are likely to be
430 involved in the host defence response against the parasite during the interaction. Moreover, this
431 response of the immune cells appears to be exacerbated in the allopatric interaction when compared to
432 the sympatric interaction.
433
434 ***Schistosoma growth and development in Biomphalaria tissues***
435 Parasite development
436 To investigate the development of *S. mansoni* in *B. glabrata* tissues, we examined the fate of
437 sporocyst in sympatric and allopatric compatible interactions using a histological approach. For both
438 interactions, miracidia were able to penetrate, transform into primary sporocysts (SpI), and develop.
439 At 24 h after infection, we observed a significant difference (Mann Whitney U test: U=40; z=4.33; p =
440 1.42 e10^{-6}) in the size of sporocyst from sympatric parasites (11,838 μm^2 average size) versus
441 allopatric parasites (7,402 μm^2 average size) (fig. 5). This difference was no longer seen 96 h after
442 infection (41,413 μm^2 and 36,920 μm^2, respectively, Mann Whitney U test: U=280; z=-1.31; p =
443 0.1917) (fig. 5). These results show that during the early events following infection, the parasites
444 develop more slowly in the allopatric compared to the sympatric interaction; thereafter, however, the
445 allopatric parasites catch up quickly, such that no difference is seen at 96 h post-infection (fig. 5).
446

447 Parasite transcript expression analysis

448 In order to investigate the biological responses of the parasites within their host, dual RNAseq
449 analyses allowed us to identify regulated transcripts from *Schistosoma* parasites during their intra-
450 molluscal development. The parasite RNAseq data at 24 h after infection, revealed five clusters of
451 differentially expressed genes from the sympatric (SmBRE) and the allopatric (SmVEN, Srod)
452 parasite responses (fig. 6). Cluster 1 corresponds to genes highly expressed and cluster 5 weakly
453 expressed for all parasite strains. Cluster 2 represents genes over-expressed in SmBRE versus SmVEN
454 and Srod. Cluster 3 contained genes over-expressed in SmBRE and SmVEN versus Srod and cluster 4
455 SmBRE and Srod versus SmVEN. In all clusters, the gene expression levels in SmBRE sympatric
456 parasite are always greater than in the other allopatric parasites. Blast2GO annotation helps in
457 characterizing 70% of the 351 genes shown in the five clusters (supplementary table S3). According to
458 the global Gene Ontology (GO): 70% of the annotated genes were involved in general metabolism and
459 growth, translation processes, regulation of cellular processes and RNA biosynthesis; 25% were
460 involved in molecular transport or cell organization; and 5% were involved in organism defence or
461 response to stimuli. In all these clusters, we identified 6 parasite gene products been involved in
462 parasite modulation or suppression of snail immunity. These molecules correspond to heat shock
463 proteins (fig. 6, clusters 1 and 2) (Knight *et al.*, 2015); glutathione-S-transferase, NADH
464 dehydrogenase subunit, and calreticulin (fig. 6, cluster 2) (Guillou *et al.*, 2007; Mone *et al.*, 2010;
465 Raghavan *et al.*, 2013); Alpha-2-macroglobulin (fig. 6, cluster 4) (Ryu, Park, 2009); von willebrand
466 factor type EGF with pentraxin domain (fig. 6, cluster 5) (Gilges *et al.*, 2000) (see supplementary table
467 S3). These particular genes could be involved in the strategy used by the parasite to ensure
468 immunosuppression and favour its development and growth within host tissues.

469

470 In allopatric interactions, an activation of the immune response is observed. Interestingly, allopatric
471 parasites did not over express any transcripts that could have immunosuppression function or impair
472 the activation of the immune response (fig. 6 and supplementary table S3). Furthermore, a variant of a
473 glycerol-3-phosphate acyl-transferase (Schisto_mansoni.Chr_3.5623) is highly over expressed in
474 SmVEN and Srod compared to SmBRE (cluster 1 supplementary table S3). This molecule is known to

475 participate in the biosynthesis of phosphatidic acid, itself involved in macrophage activation and
476 regulation of inflammatory signalling (Bohdanowicz *et al.*, 2013; Grkovich, Dennis, 2009). This
477 would thus indirectly enhance the cellular immune response of *Biomphalaria glabarata* against those
478 allopatric parasites.
479
480 Parasite microRNAs analysis
481 The microRNAs (miRNAs) are known as non-coding small RNA (<24nt) able to regulate gene
482 expressions. As we identified deep modifications of transcriptional or post-transcriptional activities
483 between sympatric and allopatric interactions, we investigated, *in-silico,* the potential presence of
484 *Schistosoma mansoni* miRNAs in our parasite RNAseq data. At 24 h post-infections, we identified 54
485 miRNA precursors from miRBase with high quality alignment scores against the different RNAseq
486 read libraries (naïve BgBRE, BB24, BV24, BR24). To avoid cross-species misidentifications, we
487 selected precursors that were exclusively identified in infected and never identified in uninfected
488 snails (naive BgBRE). Eleven miRNA precursors corresponding to *Schistosoma mansoni* were
489 identified (fig. 7A). Eight of the parasite miRNA precursors were specific to the Brazil-infected
490 libraries (BB24); two were specific of the Venezuela-infected libraries (BV24); and one was shared
491 across the three infected conditions (BB24, BV24 and BR24). Although we identify 49 miRNA
492 precursor sequences specific to *S. mansoni* (fig. 7B), we decided to select only miRNAs covered by
493 100% nucleotide similarity that allowed to predict 11 miRNAs in mature (eg. sma-mir-2d-3p, sma-
494 mir-190-3p) or precursor (sma-mir-8431)forms. Then, in order to identify candidate sequences that
495 could represent putative miRNA targets, we used the Miranda tool (supplementary table S4). Only
496 RNA-RNA interactions that showed good scores for pairing (>140) and enthalpy (<15 Kcal) were
497 considered. The number of targets pertaining to the differentially expressed immune-related transcripts
498 identified in Fig. 1 that were found for the identified miRNAs ranged from 2 targets for sma-mir-
499 8456,to 50 targets for sma-mir-2d of the differentially expressed immune-related transcripts identified
500 in Fig. 1.
501 The miRNAs identified under the sympatric condition (SmBRE) were predicted to target 43.5%of the
502 differentially represented immune-related transcripts identified in the RNAseq data (fig. 1B, fig. 7)

503 whereas 6.8% and 5.1% were targeted in allopatric conditions, SmVEN and Srod, respectively (figure
504 1B, fig. 7).To explain the similar prevalence between sympatric and allopatric infections we focus our
505 attention on miRNAs that were shared between sympatric and allopatric interactions and we identified
506 one miRNA:sma-miR-190-3p (fig. 7 and supp. Table 4). This miRNA was predicted to bind 17
507 different targets among which, we identified different variants of the Fibrinogen Related Protein
508 (FREP) family and a cytotoxic/cytolytic humoral factor the biomphalysin. To go further, we look at
509 the expression of those candidates following infection. If FREP transcripts were down regulated in
510 sympatric interaction, it is not always the case in allopatry. However, interestingly all biomphalysin
511 transcripts were under-represented in sympatric and allopatric interactions. Altogether, these data
512 suggest that the parasites might hijack the host immune response using dedicated miRNAs.
513
514 ***Survival of snail following infection***
515 To examine the potential impact of allopatric or sympatric parasites on snail survival, we investigated
516 the mortality rates of infected snails over 4 months. The survival rate was significantly higher for non-
517 infected snails compared to infected snails (sympatric interaction Kaplan-Meier Log Rank test p =
518 1.39 e10^{-5} and allopatric interaction p = 0.0005). However, there was no significant difference in the
519 mortality rates of snails subjected to sympatric versus allopatric interactions: at the end of the
520 experiment, the survival rates were 72% and 65% for the allopatric and sympatric interactions,
521 respectively (Kaplan-Meier Log Rank test p = 0.243) (supplementary fig. S2).
522
523 **Discussion**
524 In the natural environment, it is assumed that the parasitic genes responsible for infectivity will evolve
525 alongside the host defence genes, resulting in adaptation of the interactions between local host and
526 parasite populations (Dybdahl, Storfer, 2003; Osnas, Lively, 2005). In this context, local/sympatric
527 parasites were expected to display greater infectiveness, reproductive success, and virulence in host
528 populations compared to foreign/allopatric parasites (Ebert, 1994; Ebert, 1998; Lively, 1989;
529 Minchella, 1985). However, in some cases this rule may be contradicted, as certain allopatric parasite-
530 host interactions have been reported to be significantly more compatibles than the corresponding

531 sympatric combinations (Greischar, Koskella, 2007; Morand *et al.*, 1996), it appears that certain
532 *Biomphalaria/Schistosoma* interactions *(Adema et al., 1997; Zhang et al., 2007)* do not fulfil the
533 "host-parasite local adaptation hypothesis"(Ebert, 1994; Ebert, 1998; Lively, 1989; Minchella, 1985),
534 in which the sympatric parasite is expected to perform better than the allopatric one.
535 Using field data, Morand et al. (1996) and Prugnolle et al. (2006) showed that although sympatric
536 parasite-host combinations of schistosomes and snails do tend to be more compatible, exceptions exist
537 wherein particular allopatric combinations are equally or significantly more compatibles. Similar
538 results were obtained when comparing the interactions of Brazilian and Guadeloupean snails versus
539 *Schistosoma* infections(Mone *et al.*, 2011). The authors found that allopatric Guadeloupean parasites
540 were not able to infect Brazilian snails; but Brazilian parasites were able to infect the allopatric
541 Guadeloupean snails. Furthermore, this work demonstrated the presence of local adaptation between
542 reactive oxygen species (ROS) and ROS scavengers in this system (Mone *et al.*, 2011). Based on these
543 observations, we propose that it would be important to develop integrative analysis to depict and
544 understand the precise molecular crosstalk (immuno-biological interactions) occurring in such highly
545 compatible sympatric and allopatric systems. Thus, dual-comparative approaches were used herein to
546 simultaneously analyze the responses of *Biomphalaria* snails and *Schistosoma* parasites into sympatric
547 or allopatric interactions displaying similar compatibilities.
548 The present RNAseq analysis demonstrated that in sympatric interaction (BB) a huge
549 immunosuppression occurs. Twenty-four hours after the infection, the three immunological processes:
550 (i) immune recognition, (ii) effector and (iii) signaling pathways (fig. 1 and 2) were down regulated.
551 Conversely, in allopatric interactions (BV and BR), host immune response was activated (fig. 1 and 2).
552 Differentially regulated transcripts mostly belong to immune cellular activation, migration,
553 proliferation, or differentiation (fig. 2). An EdU labelling was used to detect proliferation and to
554 confirm that more hemocyte proliferation was observed in allopatry compared to sympatry (fig. 3, 4A
555 and 4B). Using flow cytometry we demonstrated that a new hemocyte subpopulation (named P2) was
556 observed exclusively following allopatric infection at 24h (fig. 4C and 4D). P2 was EdU-positive and
557 characterized by an increased in granularity, indicating that the new P2 cell subtype could proliferate.

In Biomphalaria snails, we know 3 main hemocyte morphotypes, the Blast-like cells, the type I hyalinocytes and the granulocytes (Cavalcanti *et al.*, 2012). However, in absence of specific hemocyte markers, it is impossible to analyze which hemocyte morphotype are proliferating in our flow cytometry results (fig. 4C, D). The P2 subpopulation would thus originates from either a morphological change in an existing subset (correlating potentially with a decline in the P1 population), or represents cells that are migrating from tissues or hematopoietic organ to reach the hemolymph. Indeed P2 population reflects newly proliferated cells that present higher EdU positive cells than the P1 population (Fig. 4C, D). Further investigations will be necessary to conclude on the origin of P2 population. However, hemocyte proliferation decreased more rapidly in sympatric rather than in allopatric interactions (fig. 3 and 4). By comparing different sympatric and allopatric interactions, we demonstrate that the cellular or molecular phenotype observed refers to reciprocal evolution or adaptation rather to a simple host or parasite strain effect.

The strong immunosuppression observed in sympatric interaction compared to the immune cell activation in allopatry would certainly results in differences in the capabilities of sympatric and allopatric parasites to infect and grow in such hosts. This hypothesis was confirmed by our histological analysis of sporocyst development in snail tissues. We observed a significant difference in sporocyst size 24h after infection (fig. 5), when sympatric sporocysts were one-third bigger than allopatric sporocysts. At 96h after infection, in contrast, there was no size difference between sympatric and allopatric parasites (fig. 5). This indicates that the allopatric parasites seem to overcome this early delay in development. However, the consequences of this delay for duration of cercariae development, number of cercariae produced, cercariae infectivity and pathogenicity in vertebrate host, will deserve further investigation to conclude about a potential fitness cost between sympatric and allopatric parasites.

To go further and understand how parasites immunosuppress the host or circumvent the host immune system, we used a dual-RNAseq approach to investigate transcripts expression of the sympatric and allopatric parasite intra-molluscal stages (fig. 6). As the histological differences were solely observed at 24h after infection, we used dual-RNAseq to investigate the parasite expression patterns at the same time point of infection. Most of the parasite transcripts belonged to the processes of nucleotide

586 metabolism, transcription, translation and cell differentiation, development, and growth. We also
587 identified some transcripts with GO terms or functions related to immuno-modulation or immuno-
588 suppression (fig. 6 and supplementary table S4). Nearly all of the identified transcripts were over-
589 represented in the sympatric interaction compared to the allopatric ones. Our results therefore suggest
590 that the installation, development and growth of the parasite occurred much more rapidly in the
591 sympatric combination, as sympatric parasites seemed to interfere more efficiently with the host
592 immune system. However, RNAseq data did not give any clear information about how allopatric
593 parasites succeed in circumventing the host immune system. We thus next examined the generated
594 dual-RNAseq libraries in an effort to identify whether sympatric and/or allopatric schistosomes could
595 hijack the host immune system using microRNAs. To achieve this goal, we confronted the dual-
596 RNAseq data to the *Schistosoma mansoni* subset of miRBase to identify the presence of microRNAs
597 (miRNAs) in our datasets. miRNAs are known to regulate numerous biological processes, including
598 key immune response genes (Li *et al.*, 2017; Zawada *et al.*, 2017). Recent work has demonstrated that
599 circulating small non-coding RNAs from parasites have hijack roles against host metabolism, specially
600 in the interaction of schistosomes with their vertebrate hosts (Meningher *et al.*, 2017; Nowacki *et al.*,
601 2015; Walzer, Chi, 2017). Such non-coding RNAs could act as exogenous miRNAs to interfere with
602 or circumvent the host immune system. At 24h after infection, several differentially expressed parasite
603 miRNAs were identified. We investigated the potential role played by these miRNAs on host immune
604 response. We identified some predicted targets of such schistosome miRNAs in the *Biomphalaria*
605 immune reference transcriptome. We found that schistosome miRNAs identified in the snails 24h after
606 sympatric infection may target 43.5% of the differentially regulated immune transcripts (fig. 7). In
607 contrast, far fewer correspondences were identified for the allopatric interactions (fig. 7). The higher
608 proportion of targeted genes in the sympatric interaction may result in the observed efficient
609 immunosuppression, demonstrating a specific co-evolution or adaptation in the transcriptional
610 regulation between sympatric host and parasite. However, even if more host immune genes appeared
611 to be targeted in the sympatric combination compared to the allopatric one's (fig. 7), both sympatric
612 and allopatric interactions displayed the same phenotype of compatibility. In allopatric condition,
613 despite the activation of the snail immune response, the parasite is able to develop and succeed to

614 infect the host. This similarity in compatibility phenotype between sympatric and allopatric parasites
615 could potentially results from their ability to target host immune weapons or host genes that regulate
616 innate cellular response. In this context, we were expecting to find miRNAs shared between sympatric
617 and allopatric parasites, miRNAs that do tend to weaken the immune system. A unique miRNA was
618 found to be shared by allopatric and sympatric parasites, sma-miR-190-3p, which has been identified
619 and predicted to bind different targets among which the Fibrinogen Related Protein (FREP) and
620 biomphalysin. The FREP family members are known as pathogen recognition receptors (Adema *et al.*,
621 1997; Zhang *et al.*, 2007))**.** Moreover, FREP knockdown was associated with an increase of snail
622 compatibility toward *Schistosoma* infections (Hanington *et al.*, 2012; Jiang *et al.*, 2006). Biomphalysin
623 is a key humoral factor involved in cytotoxic/cytolytic activities against *Schistosoma* parasites with the
624 ability to bind miracidia and sporocyst surfaces (Galinier *et al.*, 2013; Tetreau *et al.*, 2017). Moreover,
625 the associate snail-transcripts to these molecules are mostly down represented in sympatric and
626 allopatric interactions. The miRNA sma-miR-190-3p is perhaps essential for parasite compatibility.
627 Parasites expressing such miRNA would thus be considered as highly virulent parasites with strong
628 infecting capabilities. By producing dedicated miRNAs, the parasites were potentially able to regulate
629 transcriptional, post-transcriptional, translational and protein stability processes that might help them
630 to subvert the snail's immune defenses.
631 Compatibility reflects the outcome of complex immunobiological interactions and depends on: (i) the
632 ability of the snail immune system to recognize and kill the parasite; and (ii) the ability of the parasite
633 to circumvent or evade the host immune response (Guillou *et al.*, 2007; Mone *et al.*, 2010; Van Der
634 Knaap, Loker, 1990). Based on the present observations, we propose that sympatric and allopatric
635 interactions trigger totally different responses. In the sympatric interaction, the parasite is able to
636 induce a host immunosuppression within the first day of infection enabling it to quickly infect the host
637 and readily begins its development. In the allopatric interaction, the parasite is not able to quickly
638 neutralize the host immune system, and as a consequence the parasite is recognized by host defense
639 system that mounts a potent immune response. The need for allopatric parasites to resist the immune
640 system seems to disrupt the activation of their developmental program during the first day of infection.
641 However, they seemed to be rapidly able to protect themselves against the host immune response and

develop normally in snail tissues 96h post-infection. Thereafter, in the medium- or long-term, there are no observable differences in the prevalence, intensity, or snail survival comparing sympatric and allopatric interactions (supplementary table S1, supplementary fig. S2).

Thus, we show that despite having similar prevalence phenotypes, sympatric and allopatric snail-*Schistosoma* interactions displayed a very different immunobiological dialogue at the molecular level. Intriguingly, these different immunobiological interactions seem to have no repercussions upon parasite growth at longer term or to host survival. As differences at the molecular level do not correspond apparently to any ecologically meaningful changes in term of fitness, it is not straightforward to demonstrate local adaptation in such systems. However, we do not know if fitness costs could affect other biological traits in sympatric and allopatric interactions, as for example sporocyst II or cercariae production, or cercariae infectivity and pathogenicity towards the vertebrate host. Demonstrating local adaptation would thus appear extremely complex and would indeed deserve further investigation. It is hard to draw the line as to when local adaptation is or is not present. However, our results argue that the differences find at the molecular level may ultimately contribute to the evolution of local adaptation at an ecological level.

Nevertheless, the ability for allopatric pathogens to adapt rapidly and efficiently to new hosts could have critical consequences on disease emergence and risk of Schistosomiasis outbreaks.

Past events of allopatric parasites reaching new areas of transmission, even in large-geographic scale dispersion, have been largely documented. The most famous example being the Schistosomiasis colonization of South America since the slave trade of the 16th-19th Centuries (Crellen *et al.*, 2016; Lockyer *et al.*, 2003). *Schistosoma* originated in Asia, reached Africa 12 to 19 million years ago (MYA), and gave rise to all *Schistosoma* species known in Africa (Lockyer *et al.*, 2003). *S. mansoni* diverged from *S. rodhaini* around 2.8MYA (Crellen *et al.*, 2016; Morgan *et al.*, 2005), and thereafter,400 to 500 years ago, colonized South America (Crellen *et al.*, 2016; Lockyer *et al.*, 2003). This colonization of South America by *S. mansoni* from Africa was rendered possible by the presence of the snail host: *Biomphalaria glabrata*. All African species of *Biomphalaria* are monophyletic and seem to have originated from paraphyletic South American clades (Campbell *et al.*, 2000; DeJong *et al.*, 2001; Theron, 2005). The ancestor of *B. glabrata* appears to have colonized Africa 1 to 5 MYA,

giving rise to all 12 species of *Biomphalaria* known today in Africa (Morgan *et al.*, 2001). In South America and Caribbean Island, *S. mansoni* infects *B. glabrata*; in Africa, it infects mostly *B. pfeifferi* and *B. alexandrina*. We found that South American *S. mansoni* parasites are highly compatible with their sympatric South American snail hosts, whereas African *S. mansoni* parasites display low compatibility phenotype with South American snail hosts (supplementary table S1). Interestingly, the South American parasites did not lose their compatibility for African snail hosts; i.e., prevalences are similar to African parasites when confronted to African snails (supplementary table S1). The recent African origin of South American *Schistosoma* parasites (introduction in South America 400 to 500 years ago) may explain that they have not diverged sufficiently in South America to lose their compatibility for African snail hosts. In this case, the transfer of allopatric parasites from Africa to South American snail hosts have be successful and result in the emergence of Schsistosomiaisi in South America.

More recently another case of compatible allopatric parasite emergence have been observed when Schistososmiasis have reach Europe (Boissier *et al.*, 2016; Boissier *et al.*, 2015). Here, humans infected in Senegal have imported a hybrid between *Schistosoma haematobium* and *Schistosoma bovis* into Corsica. In this case urogenital schistosomiasis could be introduced and easily and rapidly spread into this novel area of south Corsica because *Bulinus truncatus* the vector snail of *S. haematobium* was endemic in the Corsica Cavu River (Boissier *et al.*, 2016; Boissier *et al.*, 2015). However, this allopatric African hybrid parasite was able to adapt efficiently to the Corsican new *B. truncatus* host. If parasite hybridization can potentially have a putative role in increasing the colonization potential of such *S. haematobium*, it would be particularly interesting to analyze and depict the molecular support of such allopatric interactions to predict the potential risk of schistosomiasis outbreaks in other European areas, or other potential transmission foci.

Conclusions

If we hope to draw conclusions regarding the existence of emerging or outbreak risks, we need to develop integrative approaches to explore fine-scale patterns of host-parasite interactions. We must consider the spatial scale at which comparisons are conducted, the patterns of disease occurrence, the

population genetics, and the involvement of physiological, immunological, and molecular processes. Studying the relevant factors at the relevant timing would be of critical importance in terms of Schistosomiasis control. Understanding further, how these allopatric parasites efficiently infect host snails would be mandatory to identify markers and develop new tools to predict or to quantify risks of Schistosomiasis outbreaks.

Acknowledgements

We thank Ms. Cécile Saint-Béat, Ms. Nathalie Arancibia, and Ms. Anne Rognon for their work and diligence in helping generate some of the data described herein.

Declarations

Ethics approval and consent to participate

Our laboratory holds permit # A66040 for experiments on animals, which was obtained from the French Ministry of Agriculture and Fisheries and the French Ministry of National Education, Research, and Technology. The housing, breeding, and care of the utilized animals followed the ethical requirements of our country. The experimenter possesses an official certificate for animal experimentation from both of the above-listed French ministries (Decree # 87–848, October 19, 1987). The various protocols used in this study have been approved by the French veterinary agency of the DRAAF Languedoc-Roussillon (Direction Régionale de l'Alimentation, de l'Agriculture et de la Forêt), Montpellier, France (authorization # 007083).

Availability of data and material

The datasets generated and/or analysed during the current study are not publicly available due to ongoing analysis on transcriptome but are available from the corresponding author on reasonable request.

Raw read fastq files were submitted to the Sequence Read Archive at NCBI (http://trace.ncbi.nlm.nih.gov/Traces/sra/) under the reference PRJNA213050. The reference transcriptome is publicly available from the transcriptomic database of *Biomphalaria glabrata* at the 2ei website (http://2ei.univ-perp.fr/?page_id=89 or http://ihpe.univ-perp.fr/acces-aux-donnees/)

Competing interests

The authors declare that they have no competing interests.

Funding

This work was supported by the French National Agency for Research (ANR) through the Invimory project grant [ANR-13-JSV7-0009] to BG.

Funding agency has no role in study design, collection, analysis, and interpretation of data and in writing of the manuscript.

Authors' contributions

Conceived and designed the experiments: AP, SP, RG, DD, BG. Performed the experiments: AP, SP, CC, GMC, JFA. Analyzed the data: AP, SP, CC, RG, GMC, DD, BG. AP, RG, BG led the manuscript writing. All authors participated to manuscript writing, editing, and critical reviewing. All authors read and approved the final manuscript.

Authors' information

SP current position Welcome Trust Sanger Institute, CB10 1SA Hinxton, United Kingdom

References:

Adema CM, Hertel LA, Miller RD, Loker ES (1997) A family of fibrinogen-related proteins that precipitates parasite-derived molecules is produced by an invertebrate after infection. *Proc Natl Acad Sci U S A* **94**, 8691-8696.

Baeza Garcia A, Pierce RJ, Gourbal B*, et al.* (2010) Involvement of the cytokine MIF in the snail host immune response to the parasite Schistosoma mansoni. *PLoS Pathogens* **6**, e1001115.

Bankers L, Fields P, McElroy KE*, et al.* (2018) Genomic evidence for population-specific responses to co-evolving parasites in a New Zealand freshwater snail. *Mol Ecol* **26**, 3663-3675.

Basch PF (1976) Intermediate host specificity in Schistosoma mansoni. *Experimental Parasitology* **39**, 150-169.

Bender RC, Goodall CP, Blouin MS, Bayne CJ (2007) Variation in expression of Biomphalaria glabrata SOD1: a potential controlling factor in susceptibility/resistance to Schistosoma mansoni. *Dev Comp Immunol* **31**, 874-878.

Bohdanowicz M, Schlam D, Hermansson M*, et al.* (2013) Phosphatidic acid is required for the constitutive ruffling and macropinocytosis of phagocytes. *Molecular Biology of the Cell* **24**, 1700-1712, S1701-1707.

Boissier J, Grech-Angelini S, Webster BL*, et al.* (2016) Outbreak of urogenital schistosomiasis in Corsica (France): an epidemiological case study. *The Lancet Infectious Diseases* **16**, 971-979.

Boissier J, Mone H, Mitta G*, et al.* (2015) Schistosomiasis reaches Europe. *The Lancet Infectious Diseases* **15**, 757-758.

Bonner KM, Bayne CJ, Larson MK, Blouin MS (2012) Effects of Cu/Zn superoxide dismutase (sod1) genotype and genetic background on growth, reproduction and defense in Biomphalaria glabrata. *PLoS Negl Trop Dis* **6**, e1701.

Bridger JM, Arican-Gotkas HD, Foster HA*, et al.* (2014) The non-random repositioning of whole chromosomes and individual gene loci in interphase nuclei and its relevance in disease, infection, aging, and cancer. *Adv Exp Med Biol* **773**, 263-279.

Campbell G, Jones CS, Lockyer AE*, et al.* (2000) Molecular evidence supports an african affinity of the neotropical freshwater gastropod, Biomphalaria glabrata, say 1818, an intermediate host for Schistosoma mansoni. *Proceedings of the Royal Society B* **267**, 2351-2358.

Cavalcanti MG, Filho FC, Mendonca AM*, et al.* (2012) Morphological characterization of hemocytes from Biomphalaria glabrata and Biomphalaria straminea. *Micron* **43**, 285-291.

Crellen T, Allan F, David S*, et al.* (2016) Whole genome resequencing of the human parasite Schistosoma mansoni reveals population history and effects of selection. *Sci Rep* **6**, 20954.

DeJong RJ, Morgan JA, Paraense WL*, et al.* (2001) Evolutionary relationships and biogeography of Biomphalaria (Gastropoda: Planorbidae) with implications regarding its role as host of the human bloodfluke, Schistosoma mansoni. *Mol Biol Evol* **18**, 2225-2239.

Dheilly NM, Duval D, Mouahid G*, et al.* (2015) A family of variable immunoglobulin and lectin domain containing molecules in the snail Biomphalaria glabrata. *Dev Comp Immunol* **48**, 234-243.

797 Dybdahl MF, Storfer A (2003) Parasite local adaptation: Red Queen versus suicide king.
798 *TRENDs in Ecology and Evolution* **18**, 523-530.
799 Ebert D (1994) Virulence and local adaptation of horizontally transmitted parasite. *Science*
800 **265**, 1084-1086.
801 Ebert D (1998) Experimental evolution of parasites. *Science* **282**, 1432-1435.
802 Enright AJ, John B, Gaul U*, et al.* (2003) MicroRNA targets in Drosophila. *Genome Biology* **5**,
803 R1.
804 Frank SA (1996) Models of parasite virulence. *Q Rev Biol* **71**, 37-78.
805 Galinier R, Portela J, Mone Y*, et al.* (2013) Biomphalysin, a new beta pore-forming toxin
806 involved in Biomphalaria glabrata immune defense against Schistosoma mansoni.
807 *PLoS Pathogens* **9**, e1003216.
808 Galinier R, Roger E, Mone Y*, et al.* (2017) A multistrain approach to studying the mechanisms
809 underlying compatibility in the interaction between Biomphalaria glabrata and
810 Schistosoma mansoni. *PLoS Negl Trop Dis* **11**, e0005398.
811 Gilges D, Vinit MA, Callebaut I*, et al.* (2000) Polydom: a secreted protein with pentraxin,
812 complement control protein, epidermal growth factor and von Willebrand factor A
813 domains. *Biochemical Journal* **352 Pt 1**, 49-59.
814 Goodall CP, Bender RC, Brooks JK, Bayne CJ (2006) Biomphalaria glabrata cytosolic
815 copper/zinc superoxide dismutase (SOD1) gene: association of SOD1 alleles with
816 resistance/susceptibility to Schistosoma mansoni. *Mol Biochem Parasitol* **147**, 207-
817 210.
818 Greischar MA, Koskella B (2007) A synthesis of experimental work on parasite local
819 adaptation. *Ecol Lett* **10**, 418-434.
820 Grkovich A, Dennis EA (2009) Phosphatidic acid phosphohydrolase in the regulation of
821 inflammatory signaling. *Advances in Enzyme Regulation* **49**, 114-120.
822 Guillou F, Roger E, Mone Y*, et al.* (2007) Excretory-secretory proteome of larval Schistosoma
823 mansoni and Echinostoma caproni, two parasites of Biomphalaria glabrata. *Mol*
824 *Biochem Parasitol*.
825 Hahn UK, Bender RC, Bayne CJ (2001) Involvement of nitric oxide in killing of Schistosoma
826 mansoni sporocysts by hemocytes from resistant Biomphalaria glabrata. *Journal of*
827 *Parasitology* **87**, 778-785.
828 Hanington PC, Forys MA, Loker ES (2012) A somatically diversified defense factor, FREP3, is a
829 determinant of snail resistance to schistosome infection. *PLoS Negl Trop Dis* **6**, e1591.
830 Ittiprasert W, Knight M (2012) Reversing the resistance phenotype of the Biomphalaria
831 glabrata snail host Schistosoma mansoni infection by temperature modulation. *PLoS*
832 *Pathogens* **8**, e1002677.
833 Ittiprasert W, Miller A, Myers J*, et al.* (2010) Identification of immediate response genes
834 dominantly expressed in juvenile resistant and susceptible Biomphalaria glabrata
835 snails upon exposure to Schistosoma mansoni. *Molecular and Biochemical*
836 *Parasitology* **169**, 27-39.
837 Ittiprasert W, Nene R, Miller A*, et al.* (2009) Schistosoma mansoni infection of juvenile
838 Biomphalaria glabrata induces a differential stress response between resistant and
839 susceptible snails. *Experimental Parasitology* **123**, 203-211.
840 Jiang Y, Loker ES, Zhang SM (2006) In vivo and in vitro knockdown of FREP2 gene expression
841 in the snail Biomphalaria glabrata using RNA interference. *Dev Comp Immunol* **30**,
842 855-866.

843 Kalbe M, Eizaguirre C, Scharsack JP, Jakobsen PJ (2016) Reciprocal cross infection of
844 sticklebacks with the diphyllobothriidean cestode Schistocephalus solidus reveals
845 consistent population differences in parasite growth and host resistance. *Parasit*
846 *Vectors* **9**, 130.
847 Kawecki T, Ebert D (2004) Conceptual issues in local adaptation. *Ecology letters* **7**, 1225-
848 1241.
849 Kincaid-Smith J, Rey O, Toulza E, Berry A, Boissier J (2017) Emerging Schistosomiasis in
850 Europe: A Need to Quantify the Risks. *Trends in Parasitology* **33**, 600-609.
851 Knight M, Elhelu O, Smith M*, et al.* (2015) Susceptibility of Snails to Infection with
852 Schistosomes is influenced by Temperature and Expression of Heat Shock Proteins.
853 *Epidemiology* **5**, pii: 189. Epub.
854 Larson MK, Bender RC, Bayne CJ (2014) Resistance of Biomphalaria glabrata 13-16-R1 snails
855 to Schistosoma mansoni PR1 is a function of haemocyte abundance and constitutive
856 levels of specific transcripts in haemocytes. *International Journal for Parasitology* **44**,
857 343-353.
858 Li S, Shen L, Sun L*, et al.* (2017) Small RNA-Seq analysis reveals microRNA-regulation of the
859 Imd pathway during Escherichia coli infection in Drosophila. *Dev Comp Immunol* **70**,
860 80-87.
861 Lively CM (1989) Adaptation by a Parasitic Trematode to Local Populations of Its Snail Host.
862 *Evolution* **43(8)**.
863 Lockyer AE, Emery AM, Kane RA*, et al.* (2012) Early differential gene expression in
864 haemocytes from resistant and susceptible Biomphalaria glabrata strains in response
865 to Schistosoma mansoni. *PLoS One* **7**, e51102.
866 Lockyer AE, Noble LR, Rollinson D, Jones CS (2004) Schistosoma mansoni: resistant specific
867 infection-induced gene expression in Biomphalaria glabrata identified by fluorescent-
868 based differential display. *Experimental Parasitology* **107**, 97-104.
869 Lockyer AE, Olson PD, Ostergaard P*, et al.* (2003) The phylogeny of the Schistosomatidae
870 based on three genes with emphasis on the interrelationships of Schistosoma
871 Weinland, 1858. *Parasitology* **126**, 203-224.
872 Lockyer AE, Spinks JN, Walker AJ*, et al.* (2007) Biomphalaria glabrata transcriptome:
873 identification of cell-signalling, transcriptional control and immune-related genes
874 from open reading frame expressed sequence tags (ORESTES). *Developmental and*
875 *Comparative Immunology* **31**, 763-782.
876 Meningher T, Lerman G, Regev-Rudzki N*, et al.* (2017) Schistosomal MicroRNAs Isolated
877 From Extracellular Vesicles in Sera of Infected Patients: A New Tool for Diagnosis and
878 Follow-up of Human Schistosomiasis. *Journal of Infectious Diseases* **215**, 378-386.
879 Minchella DJ (1985) Host life-history variation in response to parasitism. *Parasitology* **90**,
880 205-216.
881 Mitta G, Adema CM, Gourbal B, Loker ES, Theron A (2012) Compatibility polymorphism in
882 snail/schistosome interactions: From field to theory to molecular mechanisms. *Dev*
883 *Comp Immunol* **37**, 1-8.
884 Mitta G, Gourbal B, Grunau C*, et al.* (2017) The Compatibility Between Biomphalaria glabrata
885 Snails and Schistosoma mansoni: An Increasingly Complex Puzzle. *Adv Parasitol* **97**,
886 111-145.
887 Mone Y, Gourbal B, Duval D*, et al.* (2010) A large repertoire of parasite epitopes matched by
888 a large repertoire of host immune receptors in an invertebrate host/parasite model.
889 *PLoS Negl Trop Dis* **4**.

890 Mone Y, Ribou AC, Cosseau C*, et al.* (2011) An example of molecular co-evolution: reactive
891 oxygen species (ROS) and ROS scavenger levels in Schistosoma
892 mansoni/Biomphalaria glabrata interactions. *International Journal for Parasitology*
893 **41**, 721-730.
894 Morand S, Manning SD, Woolhouse ME (1996) Parasite-host coevolution and geographic
895 patterns of parasite infectivity and host susceptibility. *Proceedings of the Royal*
896 *Society B* **263**, 119-128.
897 Morgan JA, Dejong RJ, Adeoye GO*, et al.* (2005) Origin and diversification of the human
898 parasite Schistosoma mansoni. *Mol Ecol* **14**, 3889-3902.
899 Morgan JA, Dejong RJ, Snyder SD, Mkoji GM, Loker ES (2001) Schistosoma mansoni and
900 Biomphalaria: past history and future trends. *Parasitology* **123 Suppl**, S211-228.
901 Myers J, Ittiprasert W, Raghavan N, Miller A, Knight M (2008) Differences in cysteine
902 protease activity in Schistosoma mansoni-resistant and -susceptible Biomphalaria
903 glabrata and characterization of the hepatopancreas cathepsin B Full-length cDNA.
904 *Journal of Parasitology* **94**, 659-668.
905 Nelson MK, Cruz BC, Buena KL, Nguyen H, Sullivan JT (2016) Effects of abnormal temperature
906 and starvation on the internal defense system of the schistosome-transmitting snail
907 Biomphalaria glabrata. *J Invertebr Pathol*.
908 Nowacki FC, Swain MT, Klychnikov OI*, et al.* (2015) Protein and small non-coding RNA-
909 enriched extracellular vesicles are released by the pathogenic blood fluke
910 Schistosoma mansoni. *Journal of Extracellular Vesicles* **4**, 28665.
911 Osnas EE, Hurtado PJ, Dobson AP (2015) Evolution of pathogen virulence across space during
912 an epidemic. *Am Nat* **185**, 332-342.
913 Osnas EE, Lively CM (2004) Parasite dose, prevalence of infection and local adaptation in a
914 host-parasite system. *Parasitology* **128**, 223-228.
915 Osnas EE, Lively CM (2005) Immune response to sympatric and allopatric parasites in a snail-
916 trematode interaction. *Frontiers in Zoology* **2**, 8.
917 Penczykowski RM, Laine AL, Koskella B (2015) Understanding the ecology and evolution of
918 host-parasite interactions across scales. *Evol Appl* **9**, 37-52.
919 Perrin C, Lepesant JM, Roger E*, et al.* (2012) Schistosoma mansoni mucin gene (SmPoMuc)
920 expression: epigenetic control to shape adaptation to a new host. *PLoS Pathogens* **9**,
921 e1003571.
922 Pila EA, Gordy MA, Phillips VK*, et al.* (2016) Endogenous growth factor stimulation of
923 hemocyte proliferation induces resistance to Schistosoma mansoni challenge in the
924 snail host. *Proc Natl Acad Sci U S A* **113**, 5305-5310.
925 Pinaud S, Portela J, Duval D*, et al.* (2016) A Shift from Cellular to Humoral Responses
926 Contributes to Innate Immune Memory in the Vector Snail Biomphalaria glabrata.
927 *PLoS Pathogens* **12**, e1005361.
928 Portet A, Pinaud S, Tetreau G*, et al.* (2017) Integrated multi-omic analyses in Biomphalaria-
929 Schistosoma dialogue reveal the immunobiological significance of FREP-SmPoMuc
930 interaction. *Developmental and Comparative Immunology* **doi:**
931 **10.1016/j.dci.2017.02.025.**
932 Prugnolle F, de Meeus T, Pointier JP*, et al.* (2006) Geographical variations in infectivity and
933 susceptibility in the host-parasite system Schistosoma mansoni/Biomphalaria
934 glabrata: no evidence for local adaptation. *Parasitology* **133**, 313-319.
935 Raghavan M, Wijeyesakere SJ, Peters LR, Del Cid N (2013) Calreticulin in the immune system:
936 ins and outs. *Trends in Immunology* **34**, 13-21.

937 Richards CS (1975) Genetic factors in susceptibility of Biomphalaria glabrata for different
938 strains of Schistosoma mansoni. *Parasitology* **70**, 231-241.
939 Robertson S, Bradley JE, MacColl AD (2017) No evidence of local adaptation of immune
940 responses to Gyrodactylus in three-spined stickleback (Gasterosteus aculeatus). *Fish*
941 *and Shellfish Immunology* **60**, 275-281.
942 Roger E, Grunau C, Pierce RJ*, et al.* (2008a) Controlled Chaos of Polymorphic Mucins in a
943 Metazoan Parasite (Schistosoma mansoni) Interacting with Its Invertebrate Host
944 (Biomphalaria glabrata). *PLoS Negl Trop Dis* **2**, e330.
945 Roger E, Mitta G, Mone Y*, et al.* (2008b) Molecular determinants of compatibility
946 polymorphism in the Biomphalaria glabrata/Schistosoma mansoni model: New
947 candidates identified by a global comparative proteomics approach. *Mol Biochem*
948 *Parasitol* **157**, 205-216.
949 Ryu SJ, Park SC (2009) Targeting major vault protein in senescence-associated apoptosis
950 resistance. *Expert Opinion on Therapeutic Targets* **13**, 479-484.
951 Sminia T, Barendsen L (1980) A comparative morphological and enzyme histochemical study
952 on blood cells of the freshwater snails, *Lymnaea stagnalis*, *Biomphalaria glabrata*,
953 and *Bulinus truncatus*. *Journal of Morphology* **165**, 31-39.
954 Tack AJ, Thrall PH, Barrett LG, Burdon JJ, Laine AL (2012) Variation in infectivity and
955 aggressiveness in space and time in wild host-pathogen systems: causes and
956 consequences. *J Evol Biol* **25**, 1918-1936.
957 Tennessen JA, Theron A, Marine M*, et al.* (2015) Hyperdiverse gene cluster in snail host
958 conveys resistance to human schistosome parasites. *PLoS Genet* **11**, e1005067.
959 Tetreau G, Pinaud S, Portet A*, et al.* (2017) Specific Pathogen Recognition by Multiple Innate
960 Immune Sensors in an Invertebrate. *Front Immunol* **8**, 1249.
961 Theron A (2005) Les schistosomes et leurs hôtes : apport des marqueurs moléculaires à la
962 connaissance de leur phylogéographie, épidémiologie et écologie. *Bulletin de la*
963 *Société Zoologique de France* **130** 205-218.
964 Theron A, Pages JR, Rognon A (1997) Schistosoma mansoni: distribution patterns of
965 miracidia among Biomphalaria glabrata snail as related to host susceptibility and
966 sporocyst regulatory processes. *Experimental Parasitology* **85**, 1-9.
967 Theron A, Rognon A, Gourbal B, Mitta G (2014) Multi-parasite host susceptibility and multi-
968 host parasite infectivity: a new approach of the Biomphalaria glabrata/Schistosoma
969 mansoni compatibility polymorphism. *Infection Genetics and Evolution* **26**, 80-88.
970 Van Der Knaap WPW, Loker ES (1990) Immune mechanisms in trematod-snail interactions.
971 *Parasitology Today* **6**, 175-182.
972 Walzer KA, Chi JT (2017) Trans-kingdom small RNA transfer during host-pathogen
973 interactions: The case of P. falciparum and erythrocytes. *RNA Biology*, 1-8.
974 WHO (2010) Schistosomiasis *Fact Sheet No. 115. World Health Organisation.*
975 Zawada AM, Zhang L, Emrich IE*, et al.* (2017) MicroRNA profiling of human intermediate
976 monocytes. *Immunobiology* **222**, 587-596.
977 Zhang H, Song L, Li C*, et al.* (2007) Molecular cloning and characterization of a thioester-
978 containing protein from Zhikong scallop Chlamys farreri. *Molecular Immunology* **44**,
979 3492-3500.
980 Zhao X, Yu H, Kong L, Liu S, Li Q (2016) High throughput sequencing of small RNAs
981 transcriptomes in two Crassostrea oysters identifies microRNAs involved in osmotic
982 stress response. *Sci Rep* **6**, 22687.
983

984
985

Figure Legends

Fig. 1: Dual-RNAseq of Biomphalaria immune-related transcripts

Among the differentially represented transcripts, Blast2GO functional annotation allowed us to identify 336 transcripts that appeared to be related to the *Biomphalaria* immune response. Abbreviations and colors: blue BB, sympatric interaction between BgBRE and SmBRE; green BV, allopatric interaction between BgBRE and SmVEN; and red BR, allopatric interaction between BgBRE and Srod. For each interaction 40 whole-snails are used, 20 pooled at 24h and 20 at 96h post-infection. A) Venn diagram showing the relationships among the immune transcripts found to be differentially expressed in the sympatric and allopatric interactions. B) Clustering of differentially represented immune transcripts. Heatmap representing the profiles of the 336 differentially represented immune-related transcripts in the BB, BV, or BR interactions along the kinetic of infection (at 24 and 96 h). Each transcript is represented once and each line represents one transcript. Colors: yellow, over-represented transcripts; purple, under-represented transcripts; and black, unchanged relative to levels in control naïve snails. C) Pie chart showing the distribution of the selected immune-related transcripts across three immunological processes: immune recognition (pink), immune effectors (brown), and immune signaling (blue). For each category and interaction, the respective proportion of transcripts and the direction of the effect (over- or underexpression) are indicated.

Fig. 2: Differentially represented immune-related transcripts in sympatric and allopatric interactions.

Cumulative expression [Log2FC (fold change) from DESeq2 analysis] of the immune-related transcripts identified as being differentially represented following sympatric or allopatric infection. Transcripts were grouped into the three immunological groups described in Fig. 1, and from there into functional categories. The yellow histograms correspond to cumulatively over-represented transcripts, while the purple histograms show under-represented transcripts. The black (over-represented) and gray (under-represented) diamonds correspond to the number of transcripts analyzed in each functional category. Abbreviations: BB, BgBRE/SmBRE interaction; BV, BgBRE/SmVEN interaction; and BR, BgBRE/Srod interaction. A. Immune transcript expression at 24 h post-infection. B. Immune transcript expression at 96 h post-infection.

Fig. 3: Microscopic analyse of snail hemocyte proliferations

In vitro EdU labeling of hemocytes was conducted for sympatric and allopatric interactions A) Hemocytes were collected at 24 h post-infection for *in vitro* analysis. Confocal microscopy of EdU-labeled hemocytes from snails subjected to the allopatric BV interaction (BgBRE/SmVEN). Colors: blue, DAPI; and green, EdU. B) Microscopic counting of EdU-labeled hemocytes from naïve control snails (BgBRE) (n=1,811) and those subjected to the sympatric interaction (BB: BgBRE/SmBRE) (n=2,064) or an allopatric interaction (BV: BgBRE/SmVEN) (n=1,366) recovered from 3 individual snails by condition. Colors: green, EdU-positive cells; and blue, EdU-negative cells. Between-group differences in the percentage of proliferation were tested using a Fisher exact test, with statistical significance accepted at $p<0.05$. The “a” indicates a significant difference between the naïve and infective conditions, while “b” indicates a significant difference between the infective conditions.

Fig. 4: Flow cytometry analyse of the hemocyte response in sympatric and allopatric interactions

A) Flow cytometry was used to count *in vivo* EdU-labeled hemocytes at 24 h and 96 h after infection in sympatric and allopatric interactions. A total number of hemocytes of n=10,000were recoveredfor6 biological replicates of 3 snails. Control naïve snails (BgBRE, yellow) were compared to those subjected to the sympatric interaction (BB, BgBRE/SmBRE, blue) or an allopatric interaction (BV, BgBRE/SmVEN, green).

B) The experiment described in A was repeated using the BgVEN snail strain. Control naïve snails (BgVEN, yellow) were compared to those subjected to the sympatric interaction (VV, BgVEN/SmVEN, green) or an allopatric interaction (VB, BgVEN/SmBRE, blue).

C) FSC (forward-scattered light, representing cell size) and SSC (side-scattered light, representing cell granularity) circulating hemocyte patterns in BgBRE snails under the naïve condition (yellow) or 24 h and 96 h after infections in sympatry (BB24/96, BgBRE/SmBRE, blue) or allopatry (BV24/96, BgBRE/SmVEN, green).

D) FSC and SSC circulating hemocyte patterns in BgVEN snails under the naïve condition (yellow) or 24 h and 96 h after infections in sympatry (VV24/96, BgVEN/SmVEN, blue) or allopatry (VB24/96, BgVEN/SmBRE, green). The red dots correspond to EdU-positive hemocytes.

Between-group differences in the percentage of proliferation were tested using the Mann-Whitney U-test, with statistical significance accepted at $p<0.05$. The “a” indicates a significant difference between the naïve and infective condition, “b” indicates a significant difference between the infective conditions at 24h, and “c” indicates a significant difference between the infective conditions at 96h.

Fig. 5: Development of parasites into snail tissues

A histological approach was used to monitor parasite size along the course of snail infection. The sympatric interaction (BgBRE x SmBRE) is shown in blue, and the allopatric interaction (BgBRE x SmVEN) is shown in green. For each experimental interaction, the parasite sizes were quantified at 24 and 96 h after infection. Morpho-anatomical aspects of the parasite are depicted to highlight a potential difference in parasite survival. N=7 to 10sporocystes were used as indicated in the figure.Between-group parasite size differences were assessed using the Mann-Whitney U-test, with significance accepted at $p<0.05$ (indicated by "a" on the histograms).

Fig. 6: Clustering of intra-molluscalSchistosoma expression patterns

RNAseq library mapping enabled us to identify 351 genes expressed by *Schistosoma* parasites in *Biomphalaria* snail tissues. Colors: blue, *S. mansoni* Brazil (SmBRE); green, *S. mansoni* Venezuela (SmVEN); and red, *S. rodhaini* (Srod). The heatmap represents the profiles of the 351 genes expressed by the different parasites at 24 h after infection. Each transcript is represented once and each line represents one transcript. The expression level is highlighted by the different shades of blue.

Fig. 7: In-silico identification of parasite miRNAs

miRNAs were assessed using libraries obtained from naïve snails and snails infected for 24 h under the various interaction conditions (BB24, BgBRE x SmBRE; BV24, BgBRE x SmVEN; BR24, BgBRE x Srod). A) Table highlighting the precursor miRNAs that may have targets among the immune-related snail transcripts selected in the present work. They include eight precursors specifically recovered in BB24, two in BV24, and one shared across the three infected conditions. The total numbers of potential targets in each condition are indicated. B) Venn diagram showing the potential targets according to the sympatric or allopatric interactions. Shown is an example miRNA stem-loop precursor that presents the highest number of potential host targets.

Supplementary fig. S1: Clustering of all differential represented transcripts

Clustering of differentially represented transcripts. Heatmap representing the profiles of the 1,895 differentially represented immune-related transcripts in the BB, BV, or BR interactions along the time course of infection (at 24 and 96 h). Each transcript is represented once and each line represents one transcript. Colors: yellow, over-represented transcripts; purple, under-represented transcripts; and black, unchanged relative to levels in control naïve snails.

1

Supplementary fig. S2: Mortality of B. glabrata snails after infections

The survival rates of *B. glabrata* subjected to infection by different *S. mansoni* strains were observed over 14 weeks. Kaplan Meier graphs were generated using xlstat, and the log-rank test ($p < 0.05$) was used to test for significant between-group differences. Colored curves indicate the mortality rates of naïve snails (yellow) (n=60), snails infected by the sympatric parasite (BB, BgBRE/SmBRE, blue) (n=50), and snails infected by the allopatric parasite (BV, BgBRE/SmVEN, green) (n=50). The difference in mortality between naïve and infected snails was significant ($p<0.05$), whereas that between the two infected conditions was not ($p = 0.243$).

1085
1086
1087
1088 **Table 1:** Number of transcripts in each step of transcriptomic analysis

1089

Analysis of transcriptomic data		**Analyses of Blast2GO**	**Analyses of annotations**	
Full Transcriptome	Differentially expressed	Informative annotation	Immune Transcripts	Non Immune Transcripts
159,711	3,865	1,017	336	681

1090
1091
1092
1093

Supplementary table S1: *Biomphalaria* and *Schistosoma* compatibility between African and South-American strains

			Biomphalaria		
			glabrata		*pfeifferi*
			BRE	**VEN**	**SEN**
Schistosoma mansoni	***BRE***	**P %**	**100**	70	92
		I	**3.6**	3.5	2.9
	VEN	**P %**	100	**95**	100
		I	3.2	**3.8**	4
	SEN	**P %**	27	13	**100**
		I	1.3	1	**2.5**
Schistosoma rodhaini		**P %**	80	*NA*	*NA*
		I	2	*NA*	*NA*

The prevalence (P %: percentage of snail infected) and intensity (I: number of parasites per infected host) of infection are presented for each experimental infection. The indicated values correspond to 20 miracidia. Each pairwise combination of *Biomphalaria* (BgBRE, BgVEN, BpSEN) and *Schistosomamansoni* (SmBRE, SmVEN, SmSEN) or *SchistosomaRodhaini* (Srod) were tested for compatibility. *NA*: non-available data.

Figure 1

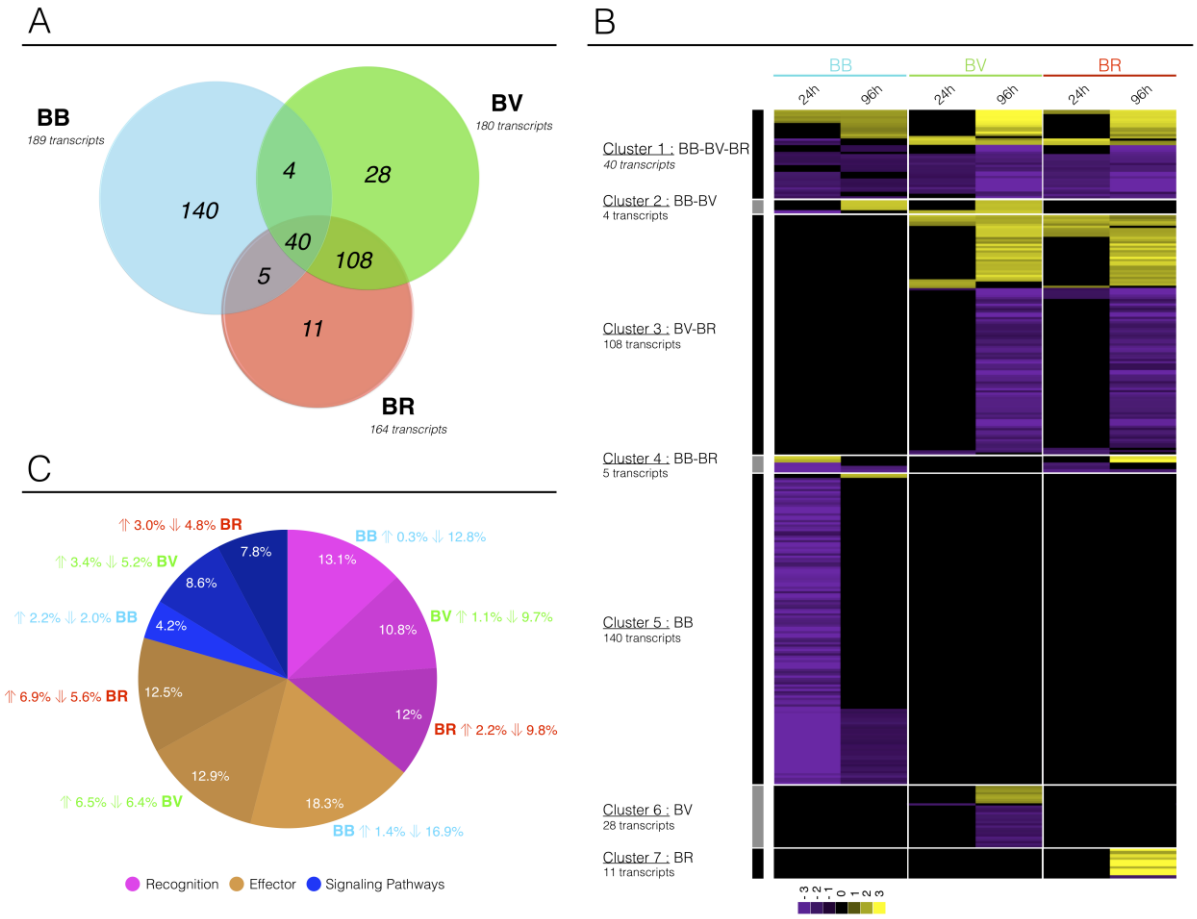
A
BB
189 transcripts
BV
180 transcripts
BR
164 transcripts
140
4
28
40
108
5
11
B
BB
BV
BR
24h
96h
Cluster 1 : BB-BV-BR
40 transcripts
Cluster 2 : BB-BV
4 transcripts
Cluster 3 : BV-BR
108 transcripts
Cluster 4 : BB-BR
5 transcripts
Cluster 5 : BB
140 transcripts
Cluster 6 : BV
28 transcripts
Cluster 7 : BR
11 transcripts
C
⇑ 3.0% ⇓ 4.8% BR
7.8%
BB ⇑ 0.3% ⇓ 12.8%
13.1%
⇑ 3.4% ⇓ 5.2% BV
8.6%
⇑ 2.2% ⇓ 2.0% BB
4.2%
BV ⇑ 1.1% ⇓ 9.7%
10.8%
⇑ 6.9% ⇓ 5.6% BR
12.5%
12%
BR ⇑ 2.2% ⇓ 9.8%
12.9%
⇑ 6.5% ⇓ 6.4% BV
18.3%
BB ⇑ 1.4% ⇓ 16.9%
Recognition
Effector
Signaling Pathways

Figure 2

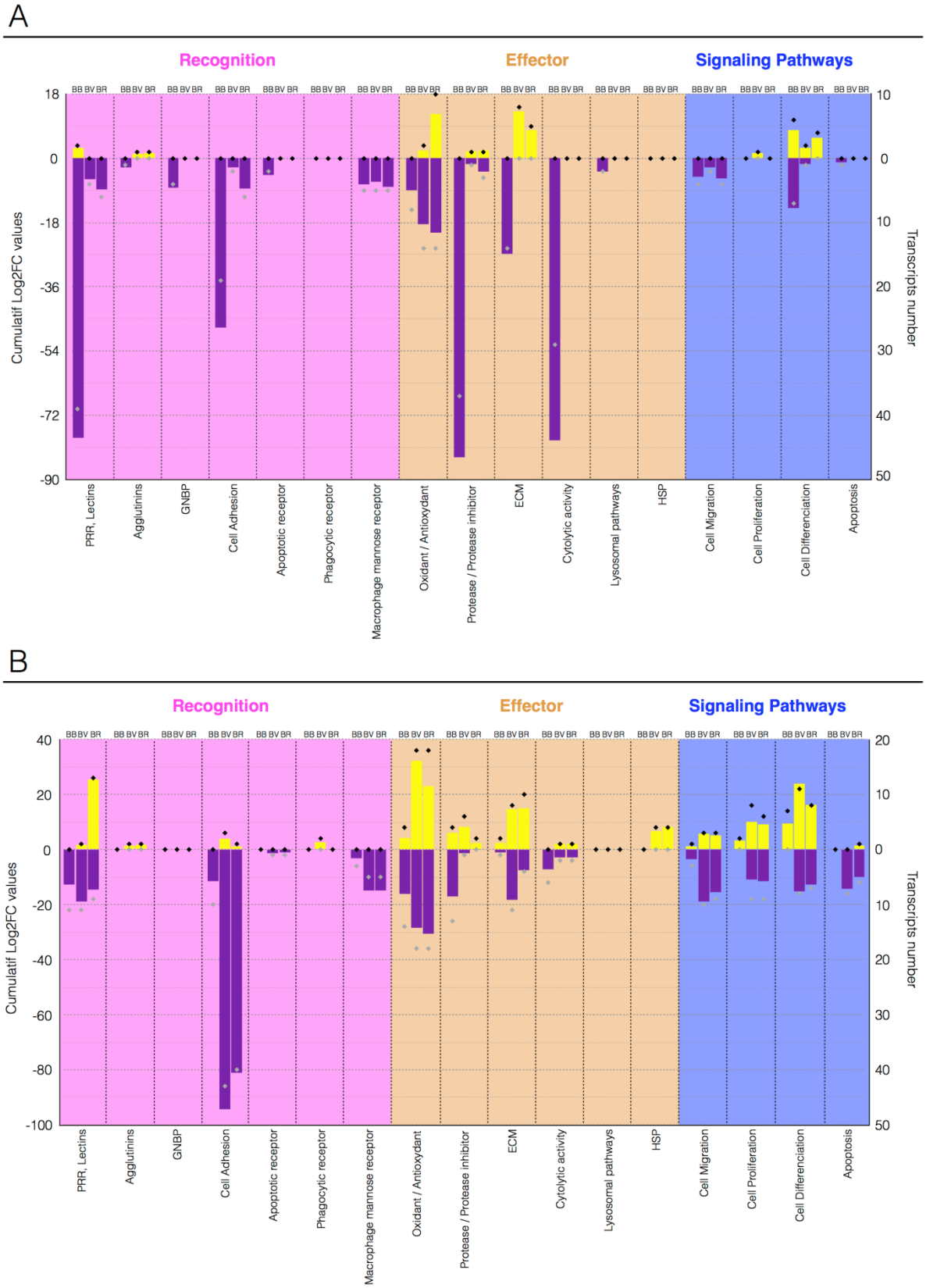
A
Recognition
Effector
Signaling Pathways
BB BV BR
Cumulatif Log2FC values
Transcripts number
PRR, Lectins
Agglutinins
GNBP
Cell Adhesion
Apoptotic receptor
Phagocytic receptor
Macrophage mannose receptor
Oxidant / Antioxydant
Protease / Protease inhibitor
ECM
Cytolytic activity
Lysosomal pathways
HSP
Cell Migration
Cell Proliferation
Cell Differenciation
Apoptosis
B
Recognition
Effector
Signaling Pathways
BB BV BR
Cumulatif Log2FC values
Transcripts number
PRR, Lectins
Agglutinins
GNBP
Cell Adhesion
Apoptotic receptor
Phagocytic receptor
Macrophage mannose receptor
Oxidant / Antioxydant
Protease / Protease inhibitor
ECM
Cytolytic activity
Lysosomal pathways
HSP
Cell Migration
Cell Proliferation
Cell Differenciation
Apoptosis

Figure 3

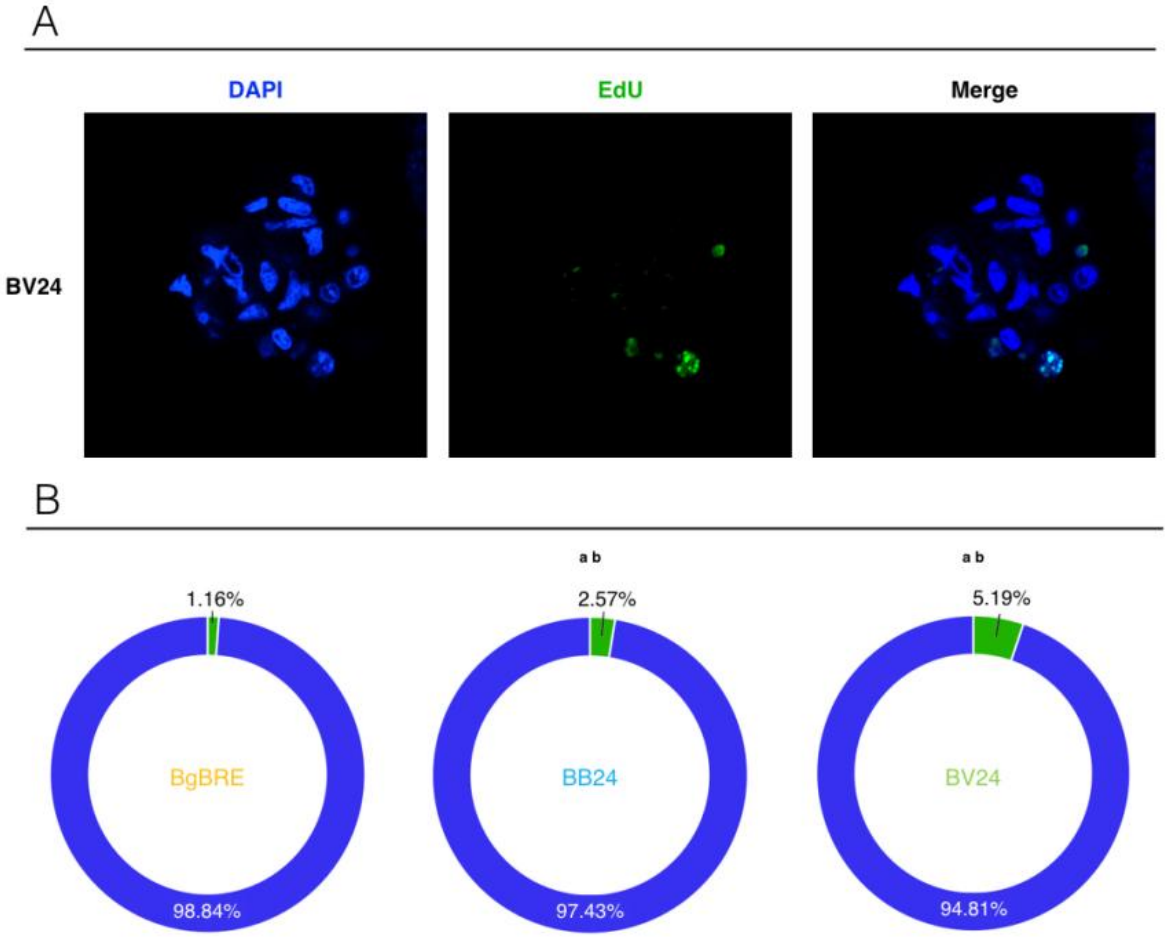
A
DAPI
EdU
Merge
BV24
B
a b
a b
1.16%
2.57%
5.19%
BgBRE
BB24
BV24
98.84%
97.43%
94.81%

Figure 4

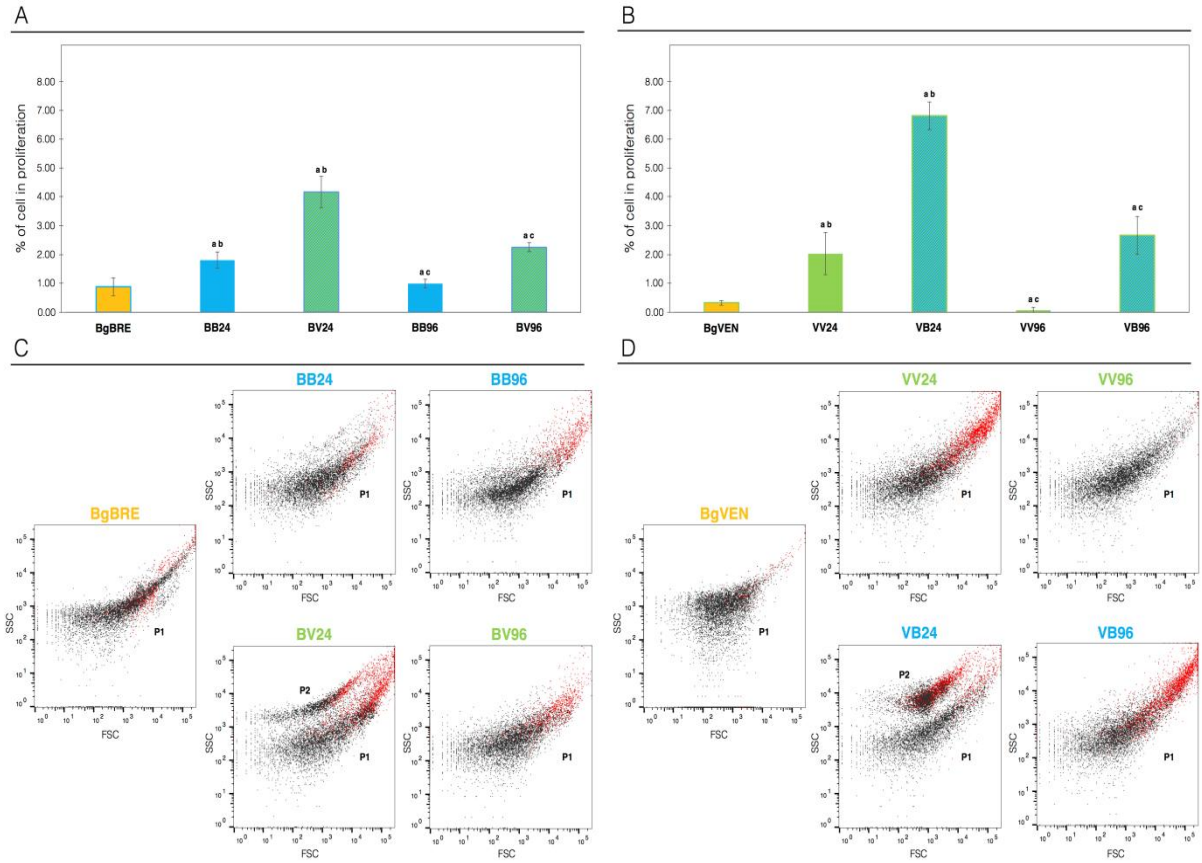
A
% of cell in proliferation
8.00
7.00
6.00
5.00
4.00
3.00
2.00
1.00
0.00
a b
a b
a c
a c
BgBRE
BB24
BV24
BB96
BV96
B
% of cell in proliferation
a b
a b
a c
a c
BgVEN
VV24
VB24
VV96
VB96
C
BgBRE
BB24
BB96
BV24
BV96
SSC
FSC
P1
P2
D
BgVEN
VV24
VV96
VB24
VB96
SSC
FSC
P1
P2

Figure 5

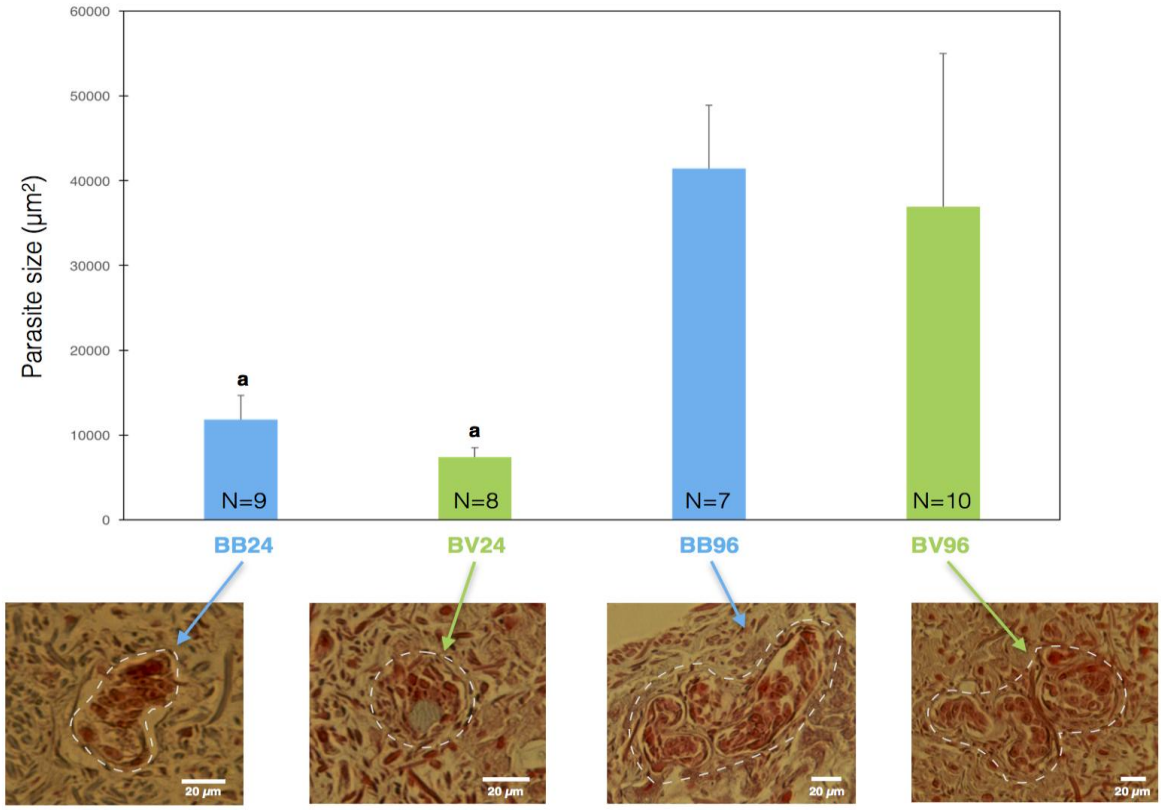
Parasite size (µm²)
60000
50000
40000
30000
20000
10000
0
a
a
N=9
N=8
N=7
N=10
BB24
BV24
BB96
BV96
20 µm
20 µm
20 µm
20 µm

Figure 6

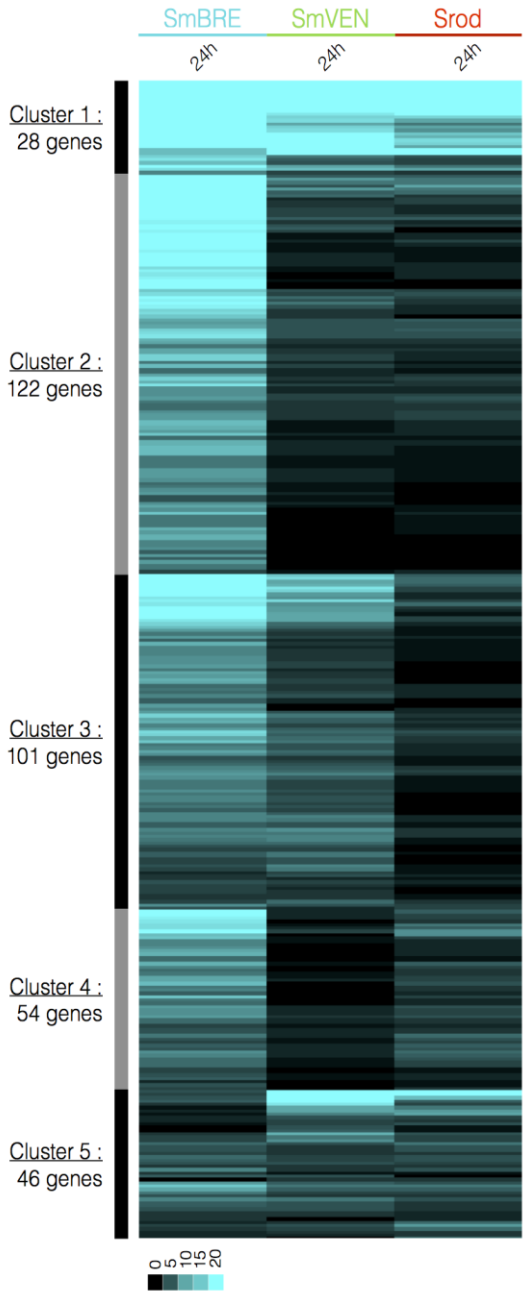
SmBRE
SmVEN
Srod
24h
24h
24h
Cluster 1 :
28 genes
Cluster 2 :
122 genes
Cluster 3 :
101 genes
Cluster 4 :
54 genes
Cluster 5 :
46 genes
0
5
10
15
20

Figure 7

A

Precursor	BgBRE duplicates		BB24	BV24	BR24	Targets
sma-mir-8460	0	0	1	0	0	7
sma-mir-8463	0	0	1	0	0	9
sma-mir-2a	0	0	1	0	0	20
sma-mir-2d	0	0	1	0	0	50
sma-mir-3492	0	0	1	0	0	10
sma-mir-8404	0	0	1	0	0	4
sma-mir-8414	0	0	1	0	0	14
sma-mir-8446	0	0	1	0	0	23
sma-mir-8456	0	0	0	1	0	2
sma-mir-8431	0	0	0	1	0	4
sma-mir-190	0	0	1	1	1	17
Sum of potential Bg targets	**0**	**0**	**154**	**23**	**17**	

SmBRE specific
SmVEN specific
Shared

B

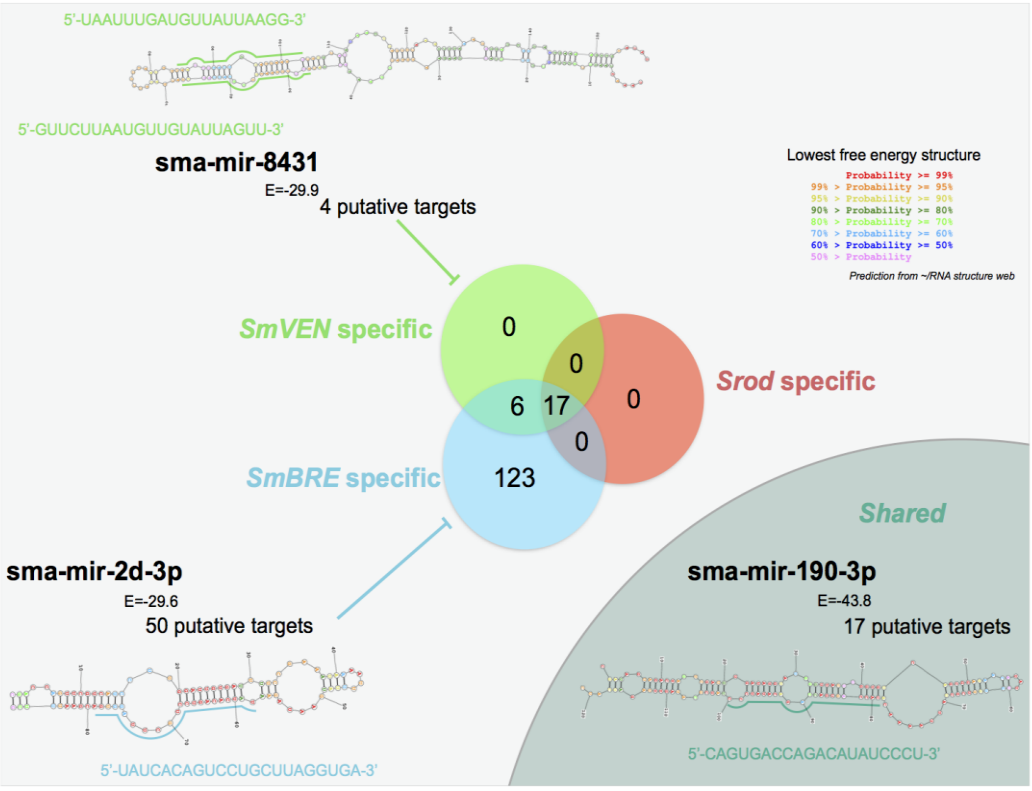

Figure S1

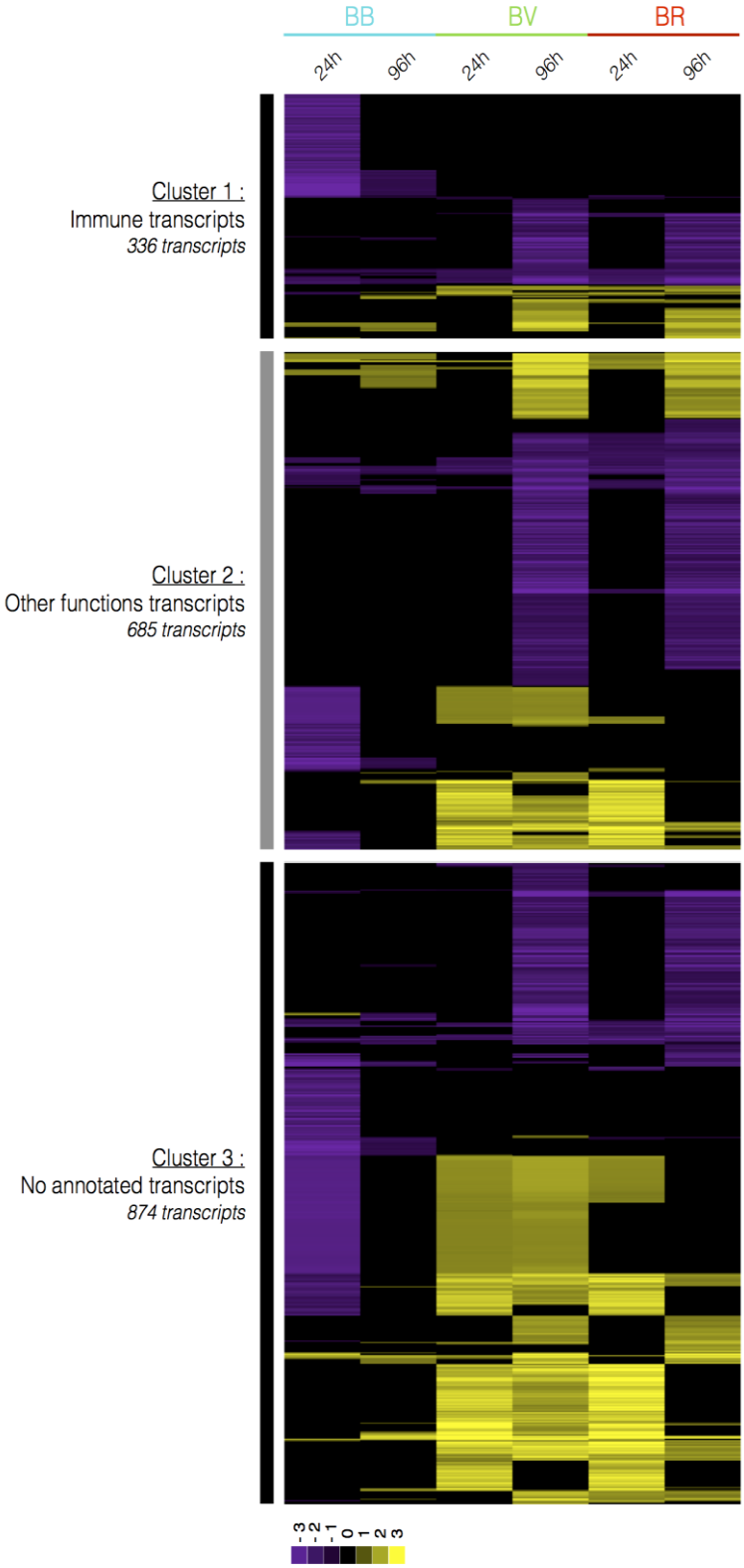
BB
BV
BR
24h
96h
24h
96h
24h
96h
Cluster 1 :
Immune transcripts
336 transcripts
Cluster 2 :
Other functions transcripts
685 transcripts
Cluster 3 :
No annotated transcripts
874 transcripts
-3
-2
-1
0
1
2
3

Figure S2

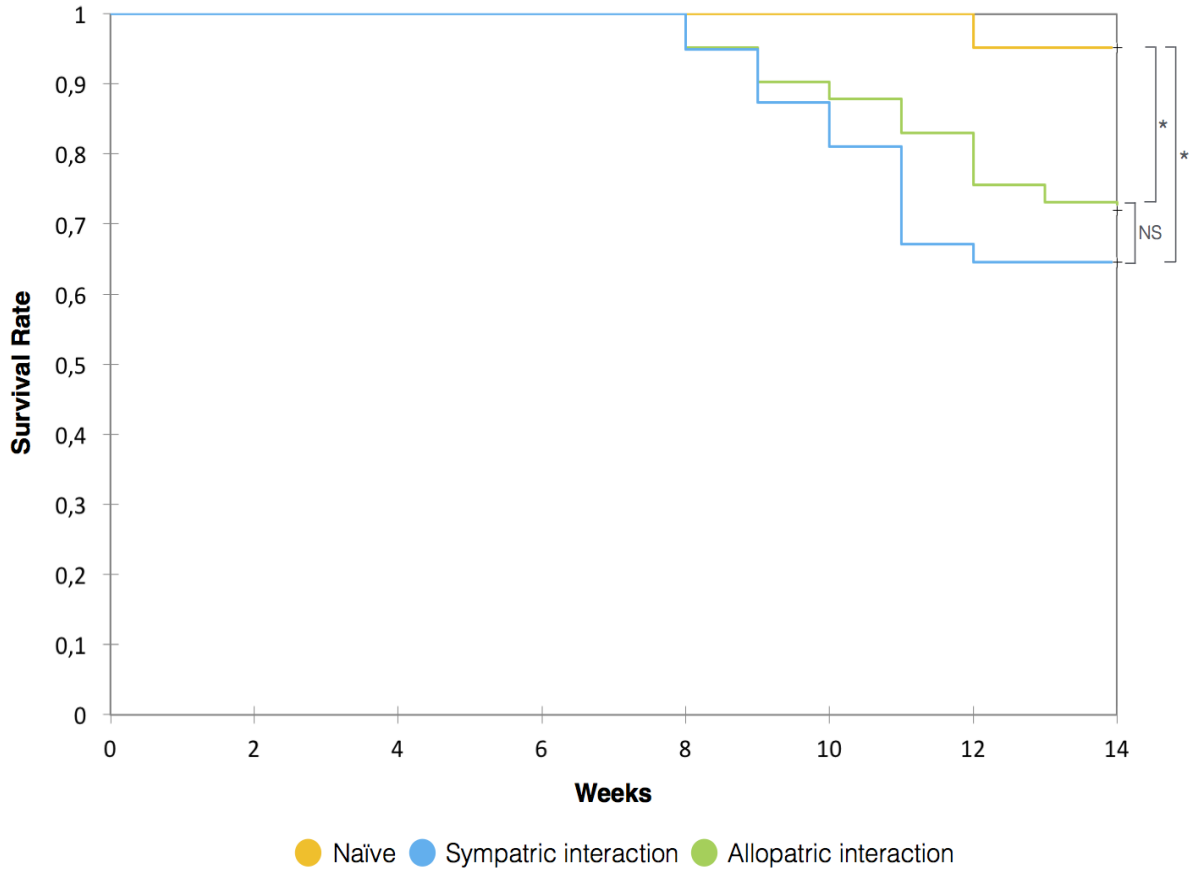
1
0,9
0,8
0,7
0,6
0,5
0,4
0,3
0,2
0,1
0
Survival Rate
0
2
4
6
8
10
12
14
Weeks
*
*
NS
Naïve
Sympatric interaction
Allopatric interaction